CHAPTER V
METHODS

5.1 Genomic DNA extraction

The genomic DNA was isolated from *R. eutropha* (TISTR 1095), *A. hydrophila* (ATCC 7966) and *P. putida* KT2440 (ATCC 47054). Bacterial colonies were resuspended in 360 µL TE buffer (100 mM Tris-HCl pH 8.0, 30 mM EDTA pH 8.0). Then, 20 µL of lysozyme (100 mg/mL) was added and incubated at 37^{o}C for 2 h. Next, 40 µL of 10% SDS was added and incubated at 55^{o}C for 30 min. One volume of phenol: chloroform: isoamyl alcohol (25 :24: 1) was added then mixed and centrifuged at 16,400 x*g* for 15 min at room temperature. The top phase was transferred to a new 1.5 mL tube and 1 volume of chloroform: isoamyl alcohol (24: 1) was added. After centrifugation at 16,400 x*g* for 15 min at room temperature, the top phase was transferred to a new 1.5 mL tube and 0.1 volume of 3 M sodium acetate was added and mixed gently. The genomic DNA was precipitated by mixing with 2 volumes of cold ethanol and kept at -20^{o}C for 30 min. The precipitated genomic DNA was collected by centrifugation at 16,400 x*g* for 30 min at 4^{o}C. Then, the DNA pellet was washed twice with 70% cold ethanol and centrifuged at 16,400 x*g* for 5 min at 4^{o}C. The DNA pellet was air dried and dissolved in 30 µL distilled water. The extracted genomic DNA solution was stored at -20^{o}C.

Spectrophotometry was used to determine the quality and concentration of DNA. The concentration of DNA was analyzed by measuring the absorbance at 260 nm (A_{260}). The purity of DNA was determined by the ratio of A_{260}/A_{280}. It should be around 1.8.

Agarose gel electrophoresis was also used to analyze the quality and concentration of DNA. Agarose gel was prepared by melting 0.8% (w/v) of agarose in 1X TAE buffer (Tris-acetate EDTA buffer; 40 mM Tris-acetate, 1 mM EDTA, pH 8.0). The melted gel was poured into a tray and allowed to set at room temperature. For electrophoresis, the DNA solution was mixed with loading dye (25% glycerol,

60 mM EDTA and 0.25% bromophenol blue) then loaded into the well of set gel and ran at a constant voltage at 100 volts in 1X TAE buffer. After running, the gel was stained by immersing in 2.5 µg/mL of ethidium bromide solution for 5 min then destained in water for 10 min. The migration of the genomic DNA was visualized on top of an ultraviolet (UV) transilluminator.

5.2 Competent cell preparation

In this study, *E. coli* strains DH5α and BL21(DE3) were used. The competent cells were prepared as described below. One colony of *E. coli* was inoculated into 5 mL of LB medium and grown at 37^{o}C with shaking at 200 rpm for 12 h. Then 1 mL of the cultured cells was inoculated into 50 mL of fresh LB medium and grown at 37^{o}C with shaking at 200 rpm until the optical density at 600 nm (OD_{600}) reached 0.45. Then cultured cells were transferred into a sterile 50 mL polypropylene centrifuge tube and chilled on ice for 10 min. The cells were collected by centrifugation at 2,500 x*g* for 10 min at 4°C. Then the supernatant was discarded. The pellet was resuspended in 10 mL of ice-cold 0.1 M $CaCl_2$ and chilled on ice for 10 min. The cells were again collected by centrifugation at 2,500 x*g* for 10 min at 4°C and resuspended in 2 mL of ice-cold 0.1 M $CaCl_2$. Sterile glycerol was added to final concentration 30% (v/v). After chilled on ice for 10 min, the competent cells were aliquot into 1.5 mL tube, snaped-frozen in liquid nitrogen and kept at -80^{o}C until used.

5.3 Construction of recombinant plasmids

5.3.1 Construction of pETDuet-*ABC*s

Oligonucleotide primers were designed based on genome sequence data of *R. eutropha*, *A. hydrophila*, and *P. putida* KT2440. The gene IDs of $phaA_{Re}$, $phaB_{Re}$, $phaC_{Re}$, $phaC_{Ah}$, $phaC2_{Pp}$, $phaJ1_{Pp}$, $phaJ4_{Pp}$, and $phaJ_{Ah}$ are 4249783, 4249784, 4250156, 4488480, 1041897, 1046178, 1045908, and 4488481, respectively.

All cloning steps are described as in Figure 5.1. β-ketothiolase gene (*phaA*) and NADPH-dependent acetoacetyl-CoA reductase (*phaB*) were designed to

cloned into MCS1 of pETDuet-1 expression vector (Fig 5.2A). *phaA* was designed to fused with His_6-tag of pETDuet-1 vector at N-terminus whereas *phaB* was designed to fused with His_6-tag at C-terminus. Specifically, *phaA* and *phaB* were PCR amplified together as one fragment from the genomic DNA of *R. eutropha*. The oligonucleotide primers including AB(F)/*EcoR*I and AB(R)/*Afl*II were used (Table 5.1A). The amount of genomic DNA and the PCR condition are as described in Tables 5.2 and 5.3, respectively. Amplified product was analyzed on agarose gel electrophoresis and DNA band corresponding to the size of target product was purified from agarose gel using QIAquick PCR Purification kit (QIAGEN, Germany). Next, the amplified gene fragment was ligated into pTZ57R/T cloning vector to create pTZ57R/T-AB_{Re}. Then the ligation reaction was transformed into *E. coli* DH5α *via* heat-shock method. Blue/white colony screening was used to determine the candidate transformants. Next, the plasmids were isolated from several transformants and subjected to sequencing. Then, PCR amplification was performed by using pTZ57R/T-AB_{Re} as template and AB(F)/*EcoR*I and ABH6(R)/AflII as primers (Table 5.1B). The amplified product was analyzed on agarose gel electrophoresis. The expected amplicon was purified from agarose gel and digested with *EcoR*I and *Afl*II restriction enzymes then purified by QIAquick PCR Purification kit (QIAGEN, German). Next, the amplified gene fragment was ligated into MCS1 of pETDuet-1 expression vector to create pETDuet-AB_{Re}. Then the ligation was transformed into *E. coli* DH5α. After the gene sequences were confirmed, the recombinant plasmids were used to transform into the expression hosts *E. coli* BL21(DE3).

Three different origins of PHA synthase genes (*phaC*s) were used in this study. They are: *phaC* of *R. eutropha* (C_{Re}), *phaC2* of *P. putida* ($C2_{Pp}$) and *phaC* of *A. hydrophila* (C_{Ah}). Each of them was designed to fuse with His_6-tag at N-terminus and cloned into MCS2 of pETDuet-1 expression vector. Specifically, each *phaC* was PCR amplified from the genomic DNA of the corresponding strains to generate the gene fragments of $phaC_{Re}$, $phaC2_{Pp}$, and $phaC_{Ah}$-H6. The oligonucleotide primers, the amount of genomic DNA and the PCR conditions are as described in Tables 5.1A, 5.2 and 5.3, respectively. The amplified product was analyzed on agarose gel electrophoresis and the band corresponding to the size of target product was purified from agarose gel using QIAquick PCR Purification kit (QIAGEN, German). Next, the

amplified gene fragments were ligated into pTZ57R/T cloning vector to create pTZ57R/T-C_{Re}, pTZ57R/T-$C2_{Pp,}$ and pTZ57R/T-C_{Ah}-H6, respectively. Then the ligation reactions were transformed into *E. coli* DH5α. Blue/white colony screening was used to determine the candidate transformant clones. Next, the plasmids were isolated from several transformants and subjected to sequencing. Then, the PCR amplification was performed by using pTZ57R/T-C_{Re} and pTZ57R/T-$C2_{Pp}$ as template. Oligonucleotide primers used in the PCR are shown in Table 5.1B. The amplified product was analyzed by agarose gel electrophoresis. Next, the amplified products, C_{Re}-H6 and $C2_{Pp}$-H6, were digested with *Mun*I/*Avr*II and *Bgl*II/*Avr*II restriction enzymes, respectively. Then the fragments were ligated into MCS2 of pETDuet-AB_{Re} to create pETDuet-$AB_{Re}C_{Re}$ and pETDuet-$AB_{Re}C2_{Pp}$, respectively. Then, to create pETDuet-$AB_{Re}C_{Ah}$, pTZ57R/T-C_{Ah}-H6 was digested with *Mun*I and *Avr*II and the C_{Ah}-H6 fragment was ligated into MCS2 of pETDuet-AB_{Re}. Next, the ligation reaction was transformed into *E. coli* DH5α. After the gene sequences were confirmed, the recombinant plasmids were used to transform into the expression hosts *E. coli* BL21(DE3).

5.3.2 Construction of pCDFDuet-*J*s

Three (*R*)-specific enoyl-CoA hydratase genes (*phaJ*s) from three different microorganisms were used in this study. They are: *phaJ1* of *P. putida* ($J1_{Pp}$), *phaJ4* of *P. putida* ($J4_{Pp}$) and *phaJ* of *A. hydrophila* (J_{Ah}). Each of them was designed to fuse with His_6-tag at the N-terminus and then cloned into MCS1 of pCDFDuet-1 expression vector (Fig 5.2B). The cloning steps were similar to the construction of pETDuet-$AB_{Re}C_{Ah}$. Specifically, $phaJ1_{Pp}$ was cloned *via* the *Bam*HI and *Hind*III sites, while $phaJ4_{Pp}$ and $phaJ_{Ah}$ were cloned *via* the *Eco*RI and *Hind*III sites. Therefore, three recombinant plasmids were created: pCDFDuet-$J1_{Pp}$, pCDFDuet-$J4_{Pp}$, and pCDFDuet-J_{Ah}.

Figure 5.1 A schematic representation of overall procedure for construction of pETDuet-*ABC*s.

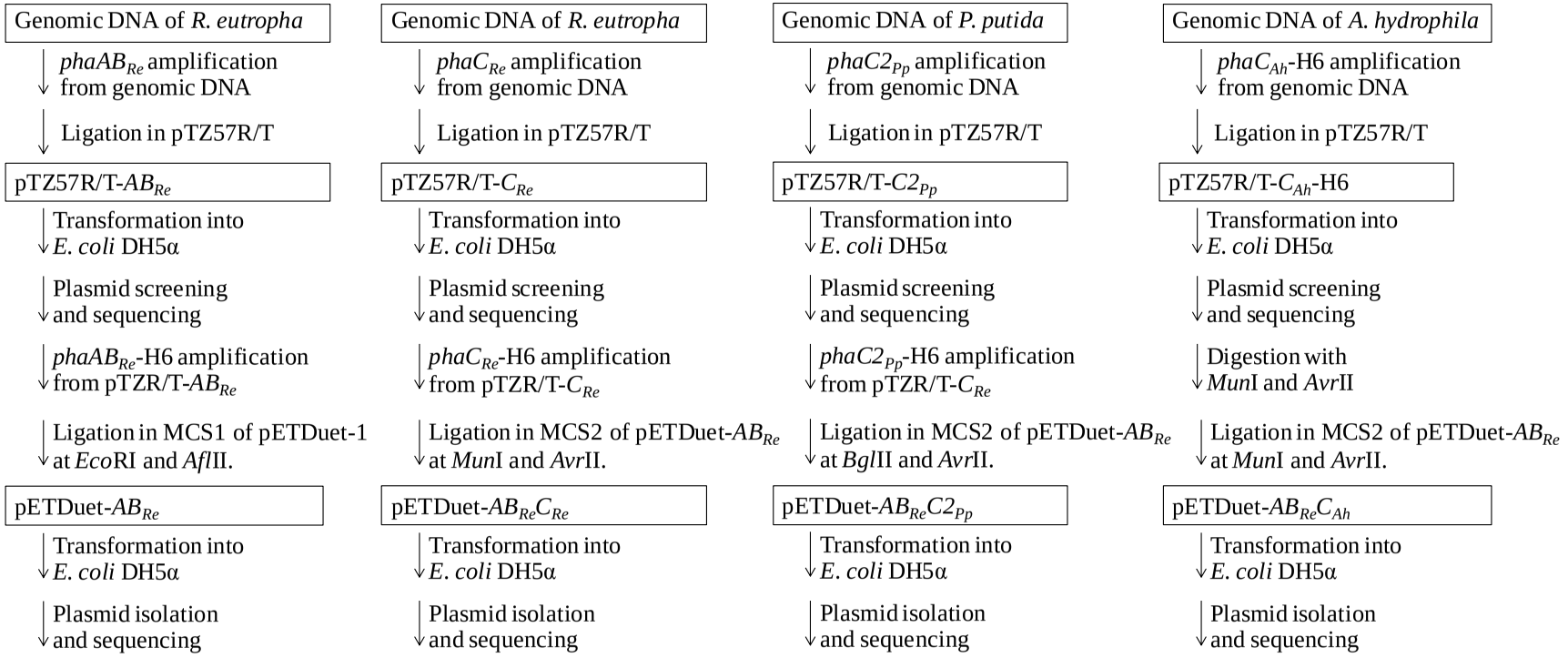

(A) (B)

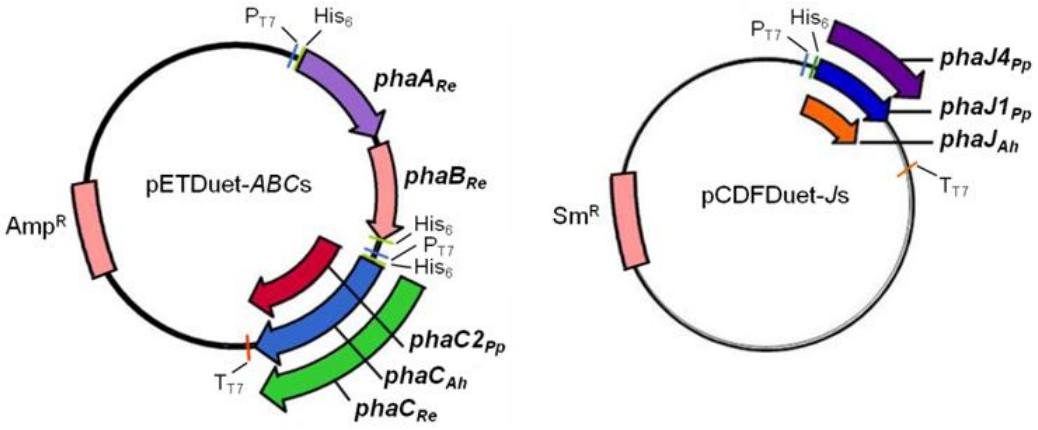

Figure 5.2 Physical map of recombinant plasmids constructed in this study. (A) pETDuet-*ABC*s and (B) pCDFDuet-*J*s. *Re*, *R. eutropha*; *Ah*, *A. hydrophila*; *Pp*, *P. putida* KT2440.

Table 5.1 (A) Oligonucleotide primers.

Target DNA	Primer name	Sequence	Length (nt)	Tm (^{o}C)
phaA and *phaB* of *R. eutropha* (*AB*$_{Re}$)	AB(F)/*Eco*RI	5’ TCTAGAATTCGACTGACGTTGTCATCGTATCCG 3’ *Eco*RI	33	63.2
	AB(R)/*Afl*II	5’ CGACCTTAAGTCAGCCCATATGCAGGCC 3’ *Afl*II	28	64.3
PhaC of A. hydrophila with His$_6$-tag (C$_{Ah}$-H$_6$)	C$_A$H6(F)/*Mun*I	5’ TCGACAATTGGCATCACCATCATCACCACAGCCAA *Mun*I His$_6$-tag TCATCTTACGG 3’	46	69.9
	C$_A$(R)/*Xma*JI	5’ AGTTCCTAGGTCATGCTGGCTCCTCCTC 3’ *Xma*JI	28	64.3
phaC of *R. eutropha* (*C*$_{Re}$)	C$_R$(F)	5’ ATGGCGACCGGCAAAGGCGC 3’	20	60.0
	C$_R$(R)	5’ TCATGCCTTGGCTTTGACGTATCGCC 3’	26	61.1
phaC2 of *P. putida* (*C2*$_{Pp}$)	C2$_P$(F)	5’ ATGACAGACAAACCGGCCAAAGGATCG 3’	27	61.3
	C2$_P$(R)	5’ TCATCGGGTCAGCACGTAGGTGCCTG 3’	26	64.3
PhaJ1 of *P. putida* (*J1*$_{Pp}$)	J1$_P$(F)/*Bam*HI	5’ GGATCCGTCCCAGGTCACCAACACGCCTTAC 3’ *Bam*HI	31	68.3
	J1$_P$(R)/*Hind*III	5’ AAGCTTTCAGCTCGCCACAAAGTTCG 3’ *Hind*III	26	59.5
PhaJ4 of *P. putida* (*J4*$_P$p)	J4$_P$(F)/*Eco*RI	5’ TCTAGAATTCGCCCCATGTACCGGTTACAGAGC 3’ *Eco*RI	33	65.6
	J4$_P$(R)/*Hind*III	5’ AGTCAAGCTTTCAGACAAAACAGAGCGACAG 3’ *Hind*III	31	61.7
PhaJ of *A. hydrophila* (*J*$_{Ah}$)	J$_A$(F)/*Eco*RI	5’ TCTAGAATTCGAGCATGCCTCCCTTCGAGGTG 3’ *Eco*RI	32	65.7
	J$_A$(R)/*Hind*III	5’AGTCAAGCTTTCAGCCGAACTTCACCACGGCTTC 3’ *Hind*III	34	66.8

Table 5.1 (B) Oligonucleotide primers (Cont.).

Target DNA	Primer name	Sequence	Length (nt)	Tm (^{o}C)
phaA and *phaB* of *R. eutropha* with His_6-tag (AB_{Re}-H_6)	AB(F)/*Eco*RI	5' TCTAGAATTCGACTGACGTTGTCATCGTATCCG 3' *Eco*RI	33	63.2
	ABH6(R)/*Afl*II	5' GTACCTTAAGTCAATGATGGTGGTGATGGTGGC *Afl*II His_6-tag CCATATGCAGGCCGCCGTT 3'	52	74.0
phaC of *R. eutropha* with His_6-tag (C_{Re}-H_6)	C_RH6(F)/*Mun*I	5' TCGACAATTGGCATCACCATCATCACCACGCGA *Mun*I His_6-tag CCGGCAAAGGCGC 3'	46	74.3
	C_R(R)/*Xma*JI	5'AGTTCCTAGGTCATGCCTTGGCTTTGACGTATC 3' *Xma*JI	33	64.4
phaC2 of *P.putida* with His_6-tag ($C2_{Pp}$-H_6)	$C2_P$H6(F)/*Bgl*II	5' ACGTAGATCTCCATCACCATCATCACCACACAG *Bgl*II His_6-tag ACAAACCGGCCAAAGG 3'	49	72.1
	$C2_P$(R)/*Xma*JI	5' GTACCCTAGGTCATCGGGTCAGCACGTAGG 3' *Xma*JI	30	67.1

Table 5.2 Genomic DNA template for target PCR fragment.

PCR fragment	Template	
	Name	Amount (ng)
phaA and *phaB* of *R. eutropha* (AB_{Re})	Genomic DNA of *R. eutropha*	1.5
phaC of *A. hydrophila* with His_6-tag (C_{Ah}-H_6)	Genomic DNA of *A. hydrophila*	400
phaC of *R. eutropha* (C_{Re})	Genomic DNA of *R. eutropha*	1.5
phaC2 of *P. putida*($C2_{Pp}$)	Genomic DNA of *P. putida*	1.5
phaJ1 of *P. putida* ($J1_{Pp}$)	Genomic DNA of *P. putida*	200
phaJ4 of *P. putida* ($J4_{Pp}$)	Genomic DNA of *P. putida*	200
phaJ of *A. hydrophila* (J_{Ah})	Genomic DNA of *A. hydrophila*	90

Table 5.3 PCR condition used for amplifying target DNA fragment.

PCR fragment	Step								Polymerase enzyme
	Pre-denaturation		Amplification				Final extention		
	(^{o}C/min)	Number of cycle	Denaturation (^{o}C/min)	Annealing (^{o}C/min)	Extension (^{o}C/min)	Number of cycle	(^{o}C/min)	Number of cycle	
phaA and *phaB* of *R. eutropha* (*AB*$_{Re}$)	94 (1)	1	94 (1)	50 (1)	72 (1:45)	30	72 (10)	1	DyNAzyme
phaA and *phaB* of *R. eutropha* with His$_6$-tag (*AB*$_{Re}$-H$_6$)	-	-	98 (0:10)	68 (2)		30	-	-	PrimeSTAR HS
PhaC of A. hydrophila with His$_6$-tag (C$_{Ah}$-H$_6$)	95 (3)	1	95 (1)	55 (1)	72 (3:30)	30	72 (5)	1	Pfu
phaC of *R. eutropha* (*C*$_{Re}$)	94 (2)	1	94 (1)	54 (1)	72 (1:45)	30	71 (10)	1	DyNAzyme
phaC of *R. eutropha* with His$_6$-tag (*C*$_{Re}$-H$_6$)	94 (2)	1	94 (1)	50 (1)	72 (1:50)	30	72 (10)	1	DyNAzyme
phaC2 of *P. putida* (*C2*$_{Pp}$)	94 (2)	1	94 (1)	65 (1)	72 (1:45)	30	72 (10)	1	DyNAzyme
phaC2 of *P. putida* with His$_6$-tag (*C2*$_{Pp}$-H$_6$)	94 (2)	1	94 (1)	50 (1)	72 (1:50)	30	72 (10)	1	DyNAzyme
PhaJ1 of *P. putida* (*J1*$_{Pp}$)	95 (5)	1	95 (1)	60 (0:30)	72 (0:20)	30	72 (10)	1	DyNAzyme
PhaJ4 of *P. putida* (*J4*$_{P}$p)	95 (3)	1	95 (1)	50 (0:30)	72 (0:30)	30	72 (10)	1	DyNAzyme
PhaJ of *A. hydrophila* (*J*$_{Ah}$)	95 (3)	1	95 (1)	53 (1)	72 (0:30)	30	72 (5)	1	DyNAzyme

5.4 Recombinant protein expression

E. coli BL21(DE3) was used as a host for protein expression and PHA production. The recombinant plasmids, pETDuet-*AB*$_{Re}$*C*$_{Re}$, pETDuet-*AB*$_{Re}$*C*$_{Ah}$, and pETDuet-*AB*$_{Re}$*C2*$_{Pp}$, were transformed into *E. coli* BL21(DE3) generating *E. coli*-AB$_{Re}$C$_{Re}$, *E. coli*-AB$_{Re}$C$_{Ah}$, and *E. coli*-AB$_{Re}$C2$_{Pp}$, respectively. The recombinant plasmids, pCDFDuet-*J1*$_{Pp}$, pCDFDuet-*J4*$_{Pp}$, and pCDFDuet-*J*$_{Ah}$ were transformed into *E. coli* BL21(DE3) generating 3 recombinant strains namely *E. coli*-J1$_{Pp}$, *E. coli*-J4$_{Pp}$, and *E. coli*-J$_{Ah}$. Moreover, the recombinant plasmids: pETDuet-*ABC*s and pCDFDuet-*J*s were co-transformed into *E. coli* BL21(DE3) generating nine recombinant strains namely *E. coli*-ABC$_{Re}$J1$_{Pp}$, *E. coli*-ABC$_{Re}$J4$_{Pp}$, *E. coli*-ABC$_{Re}$J$_{Ah}$, *E. coli*-ABC$_{Ah}$J1$_{Pp}$, *E. coli*-ABC$_{Ah}$J4$_{Pp}$, *E. coli*-ABC$_{Ah}$J$_{Ah}$, *E. coli*-ABC2$_{Pp}$J1$_{Pp}$, *E. coli*-ABC2$_{Pp}$J4$_{Pp}$, and *E. coli*-ABC2$_{Pp}$J$_{Ah}$.

To investigate the expression ability of recombinant proteins in *E. coli*, several transformant clones of each strain were cultivated in LB supplemented with appropriate antibiotics (100 µg/mL of ampicillin for *E. coli*-ABCs, and 50 µg/mL of streptomycin for *E. coli*-Js, and 50 µg/mL of ampicillin and 50 µg/mL streptomycin for *E. coli*-ABCsJs), overnight (16 h) at 37^{o}C, 200 rpm. The overnight cultures were inoculated into fresh LB containing appropriate antibiotics (5% inoculums) and cultured at 37^{o}C with shaking 200 rpm until OD_{600} reached 0.6. Isopropyl-thio-β-D-galactopyranoside (IPTG) was added to the cultures as an inducer with final concentration of 1 mM. The cell cultures were grown at the same conditions for 3 h. Then they were harvested by centrifugation. Cell pellets were directly subjected to analyze by SDS-PAGE or stored at -20^{o}C until used.

5.5 Protein analysis

5.5.1 SDS-PAGE

Protein expression profile was analyzed by SDS-PAGE. The harvested cells were mixed with 5x loading buffer [10% (w/v) SDS, 10 mM β-mercaptoethanol, 20% (v/v) glycerol, 0.2 M Tris-HCl, pH 6.8, and 0.05% (w/v) bromophenol blue). The reaction was boiled for 10 min, then vortexed. Next, it was centrifuged to obtain clear

supernatant and loaded into 12% SDS-PAGE. The ingredients for SDS-PAGE preparation is shown in Table 5.4. The protein profile was resolved in 1x Tris-glycine running buffer [25 mM Tris-HCl, 250 mM glycine and 0.1% (w/v) SDS] at constant current of 15 mA per gel. After electrophoresis, the gel was stained in staining buffer [0.25% (w/v) Coomassie Brilliant Blue R-250, 45% (v/v) methanol, and 10% (v/v) acetic acid] for 30 min with mild shaking. Then, the gel was destained in destaining solution [10% (v/v) methanol and 10% (v/v) acetic acid] with shaking until excess dye was removed.

Table 5.4 Components of SDS-PAGE for protein determination.

Preparation of 5% of stacking SDS-PAGE	
Solution	**Volume (µl)**
30% Acrylamide[a]	333
H_2O	1,500
1 M Tris-HCl pH 6.8	625
10% SDS	25
10% APS	15
TEMED	3
Total volume	2,501
Preparation of 12% of separating SDS-PAGE	
Solution	**Volume (µl)**
30% Acrylamide[a]	2,400
H_2O	2,010
1 M Tris-HCl pH 8.8	1,500
10% SDS	60
10% APS	30
TEMED	3
Total volume	6,003

[a]Acrylamide, N,N'-methylene-bis-acrylamide 29: 1 (w/w); APS, ammonium persulphate; TEMED, N,N,N',N'-tetramethyl-ethylenediamine

5.5.2 Western blot analysis

Western blot analysis was performed to verify the specificity of recombinant proteins. After the proteins were electrophoresed into 12% SDS-PAGE, the proteins on the gel were transferred to polyvinylidene difluoride (PVDF) membrane by wet-blotting. The electroblotting was performed at constant voltage of 100 volts for 90 min in 1x transfer buffer [25 mM Tris-base, 190 mM glycine, 20% (v/v) methanol, and 0.05% (v/v) SDS]. Non-specific binding was blocked with 5% skim milk in PBS, pH 7.4 (8 g/L of NaCl, 0.2 g/L of KCl, 1.44 g/L of Na_2HPO_4, and 0.24 g/L of KH_2PO_4) for 2 h then washed by PBST [PBS with 0.1% (v/v) Tween-20] for 10 min. Next the membrane was probed with monoclonal anti-polyHistidine in 5% skim milk in PBS (1:3,000 dilutions) for 1 h. The membrane was washed 3 times with PBST for 10 min each then probed with secondary antibody, anti-Mouse IgG (whole molecules)-alkaline phosphatase in 5% skim milk in PBS (1:30,000 dilution) for 2 h. Then, the membrane was washed once with PBST for 10 min and twice more with PBS for 10 min each. The membrane was incubated in the colorimetric detection solutions, 5-bromo-4-chloro-3-indolyl phosphate and *p*-nitroblue tetrazolium chloride (BCIP/NBT) substrate, for 30 min.

5.6 Crude glycerol characterization

Crude glycerol used in this study was obtained from a local biodiesel production plant (Trang Palm Oil Co. Ltd., Trang, Thailand) which was the by-product of alkaline (NaOH)-catalyzed transesterification of palm oil with methanol. Methanol in the crude glycerol was quantified using a gas chromatograph GC-6850 equipped with a flame ionization detector and a HP-Innowax column (30 m x 0.32 mm I.D. x 0.25 µm film thickness) (Hewlett Packard, Santa Clara, CA). Glycerol and mono-/di-/tri-glycerides were measured using a gas chromatograph GC-2010 (d) equipped with a flame ionization detector and a type DB-1HT column (10 m x 0.32 mm I.D. x 0.1 micron film thickness) (Agilent, Santa Clara, CA). Sodium and potassium were quantified by atomic absorption chromatography operated by the Department of Science Service (Bangkok, Thailand).

5.7 PHA production

5.7.1 Culture media and conditions

5.7.1.1 P(3HB) biosynthesis

M9 minimum medium (136) with or without Bacto-yeast extract (1 g/L) containing pure or crude glycerol as sole carbon source was used as culture media. To maintain the plasmids, ampicillin (100 mg/L) and ampicillin (100 mg/L) together with streptomycin (50 mg/L) were supplemented into the media for cultivation of *E. coli*-ABCs and *E. coli*-ABCsJs, respectively. The colonies on an agar plate were pre-culture in LB medium at 37^{o}C for 15 h at 200 rpm on a rotary shaker. Then this pre-culture was inoculated into 75 or 300 mL PHA production medium which was in 250 or 1000 mL flask at an inoculums volume of 0.15 OD/mL. The cultured cells were incubated at 37^{o}C with rotary shaking at 200 rpm. IPTG (1mM) was added to the media to induce protein expression after 3 h or 6 h of cultivation and further incubating for 24-48 h. The cultured cells were harvested by centrifugation and dried at 65^{o}C. Cell growth was measured by OD_{600} and the amount of dried cell was weighted. Protein expression was analyzed by SDS-PAGE (the method was described above).

5.7.1.2 SCL-MCL-PHAs biosynthesis

M9 minimum medium (136) with Bacto-yeast extract (1 g/L) containing pure or crude glycerol as sole carbon source was used as culture media. To maintain the plasmids, ampicillin (100 mg/L) and ampicillin (100 mg/L) together with streptomycin (50 mg/L) were supplemented into the media for cultivation of *E. coli*-ABCs and *E. coli*-ABCsJs, respectively. The colonies on an agar plate were pre-culture in LB medium at 37^{o}C for 15 h at 200 rpm on a rotary shaker. Then this pre-culture was inoculated into 75 or 300 mL PHA production medium which was in 250 or 1000 mL flask at an inoculums volume of 0.15 OD/mL. The cultured cells were incubated at 37^{o}C with rotary shaking at 200 rpm. Sodium dodecanoate (0.5-1.5 g/L), Brij-35 (2 g/L) (for solubilization of dodecanoate) (68), and IPTG (1 mM) were added to the medium after 3 h of cultivation, and the cells were grown for additional 24 h.

The cultured cells were harvested by centrifugation and dried at 65^{o}C. The cell growth was measured by OD_{600} and the amount of dried cell was weighted. Protein expression was analyzed by SDS-PAGE.

5.7.2 Analytical method

5.7.2.1 Fluorescent dye staining

Accumulation of P(3HB) granules inside the cells were detected by Nile Blue A staining analysis (137). Specifically, *E. coli* cells were heat-fix smeared on glass slide and stained with 1% (w/v) Nile blue A solution at 55^{o}C for 10 min. Then, the slide was washed with tap water and 8% (v/v) acetic acid for 1 min to remove the excess stain. The prepared slide was observed under fluorescence microscope and confocal laser scanning microscope. The excitation wave length was 460 nm.

5.7.2.2 High performance liquid chromatography

5.7.2.2.1 P(3HB) quantification

To determine the quantities of P(3HB) accumulated in the *E. coli* cells, the dried cells were hydrolytically digested by sulfuric acid (138). After hydrolysis, the hydrolyzed samples were filtrated and analyzed by high performance liquid chromatography (HPLC) on an Ultimate 3000 standard LC system (Dionex, Sunnyvale, CA) equipped with an Aminex HPX-87H (300 mm x 7.8 mm I.D., Bio-Rad, Hercules, CA). The samples were eluted with 10% CH_3CN in 5 mM H_2SO_4 at 65^{o}C at a flow rate of 0.4 mL/min. Chromatogram signals were detected at 210 nm.

5.7.2.2.2 SCL-MCL-PHAs quantification and compositions analysis

To determine the quantities and the compositions of the accumulated PHAs in *E. coli* cells, the dried cells were digested by alkaline hydrolysis with slight modification (139). Specifically, approximately 20 mg of dried

cells was treated with 1 N NaOH (1 mL) at 100^{o}C for 3 h (vortexing every 1 h) then neutralization with 1 N HCl (1 mL). The solutions were centrifuged at 21,000 *xg* for 30 min and filtrated. The filtrated samples were analyzed by HPLC on an Ultimate 3000 standard LC system (Dionex, Sunnyvale, CA) equipped with a UV detector and an Aminex HPX-87H column (300 mm x 7.8 mm I.D) (Bio-Rad, Hercules, CA) operated at 65^{o}C at a flow rate of 0.4 mL/min. The mobile phase was 10% CH_3CN in 5 mM H_2SO_4 and chromatogram signals were detected at 210 nm.

5.7.2.2.3 Glycerol quantification

The remained glycerol concentration in the media was quantified by high performance liquid chromatography (HPLC) on a Water e2695 (Milford, MA) equipped with RI detector and a Shodex sugar SH 1011 column (8.0 mmID x 300 mmL) (New York NY) operated at 60^{o}C at a flow rate of 0.6 mL/min. The mobile phase was 5 mM H_2SO_4.

5.7.2.3 PHAs extraction and purification

In order to determine the physical and thermal properties of polymers, the accumulated PHA in recombinant *E. coli* was extracted by solvent extraction method. The accumulated PHA in dried cell was extracted in chloroform at 80^{o}C for 48 h after that the chloroform was evaporated to obtain PHA film. Next, the obtained PHA film was purified by dissolving in chloroform and then precipitating in 4-fold volumes of hexane or cold methanol. The white PHA powder was obtained (Fig 5.3).

Dried cell

↓

Extraction with chloroform at 80^{o}C for 48 h

↓

Chloroform evaporation to obtain PHA film

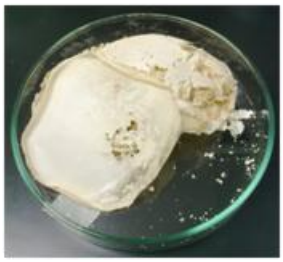

↓

Precipitation with hexane or cold methanol
to obtain purified PHA powder

Figure 5.3 PHA extraction and purification flowchart.

5.7.2.4 Nuclear magnetic resonance

To measure proton nuclear magnetic resonance (^{1}H NMR), five mg of PHA sample was dissolved in dueterated chloroform and analyzed on a Bruker AVANCE III 400 spectrometer at 400 MHz (Bruker, Helios, Singapore). To measure carbon nuclear magnetic resonance (^{13}C NMR), twenty mg of PHA sample was dissolved in dueterated chloroform and analyzed on a Bruker AVANCE III 400 spectrometer at 400 MHz (Bruker, Helios, Singapore). The chemical shift of each proton and carbon resonance was assigned relying on the chemical shift of standard P(3HB) and P(3HB-*co*-3HHx) (Nodax^{TM}).

5.7.2.5 Gel permeation chromatography

Molecular mass data on PHAs were acquired by gel permeation chromatography (GPC) analysis at 40^{o}C using a Hewlett packard 1100 series system with a refractive index detector and a varian PLgel 10 µm MIXED-B column (Fisher Scientific, Hampton, NH). Tetrahydrofuran was used as eluent at a flow rate of 1 mL/min. Polystyrene standards were used to construct a calibration curve.

5.7.2.6 Differential scanning calorimetry

Thermal properties were evaluated by differential scanning calorimetry (DSC) using a DSC 1 STAR^{e} system (Mettler Toledo, Columbus, OH). Temperature scanning was from -50^{o}C to 200^{o}C. The observed melting temperature (T_m) was obtained from the positions of the endothermic peaks. The glass transition temperature (T_g) was taken as the midpoint of heat capacity change.

5.7.2.7 Thermogravimetry analysis

The degradation temperature (T_d) was evaluated by thermogravimetry analysis (TGA) using TGA/SDTA 851^{e} (Mettler Toledo, Columbus, OH). Ten milligrams of polymers were heated at the rate of 20^{o}C/min from 30^{o}C to 500^{o}C in a nitrogen atmosphere.

CHAPTER VI
RESULTS

6.1 Establishment of PHA biosynthetic pathway in recombinant *E. coli*

In this study, we aim to investigate the biosynthesis of SCL-MCL-PHAs from glycerol by recombinant *E. coli* strains. SCL-MCL-PHAs have a wide range of applications due to their properties that can range from being thermoplastic to elastomer. These properties depend on the composition and the molar fraction between SCL-monomer and MCL-monomer. Different plastic products require different properties of plastic materials. Only a few microorganisms can produce SCL-MCL-PHAs and it is difficult to adjust the content and the compositions of copolymers produced by these bacteria as their metabolic pathways are poorly characterized and tools for genetic modification are not available. Therefore, the genetic engineering of model microorganism, *Escherichia coli*, was selected in this study. The pathway construction was divided into two main steps. First, the pathway for biosynthesis of P(3HB), employing PhaABC enzymes, was constructed in *E. coli*. Second, PhaJ was introduced into the recombinant strains to co-express with PhaABC, completing the pathway for biosynthesis of SCL-MCL-PHA copolymers.

6.1.1 Pathway design and amino acid alignment

Based on the known natural PHA biosynthesis pathways, the hybrid pathway was designed by combining two monomer-supplying pathways with one polymerization pathway. For supplying SCL-monomer, two enzymes: PhaA and PhaB of *R. eutropha* were selected to convert acetyl-CoA to (*R*)-3-hydroxybutyryl-CoA. For supplying MCL-monomers, PhaJ was selected to convert enoyl-CoA to (*R*)-3-hydroxyacyl-CoA. The designed pathway is shown in Figure 1.2.

Since variation in polymer properties leads to a wide range of applications, 3 different PhaCs and 3 different PhaJs were employed in this study to produce the

different compositions of PHAs. Three different PhaCs were selected based on their different types of PHAs produced in their native strains. These are: PhaC from *R. eutropha* (TISTR 1095) ($PhaC_{Re}$) which was previously reported as SCL-PHA producing strains (140), PhaC from *A. hydrophila* (ATCC 7966) ($PhaC_{Ah}$) which was previously reported as the SCL-MCL-PHA producing strain (31) and PhaC from *P. putida* KT2440 (ATCC 47054) ($PhaC2_{Pp}$) which was previously reported as the MCL-PHA producing strain (141). Amino acid sequence alignment was carried out to preliminary examine their identity to each other and/or to the other well characterized enzymes. By Clustal Omega alignment, amino acid sequence of $PhaC_{Re}$, $PhaC_{Ah}$, and $PhaC2_{Pp}$ showed 36-40% identity. The conserved residues presumably forming a catalytic triad are cysteine, aspartate, and histidine (29) as indicated by the arrows in Figure 6.1. Amino acid sequence of $PhaC_{Ah}$ was elucidated by genome sequence project (70) and there is no information of heterologous expression of $PhaC_{Ah}$ in recombinant *E. coli*. The amino acid sequence identity of $PhaC_{Ah}$ with the well known PhaC of *A. caviae* ($PhaC_{Ac}$) (13, 142) was as high as 92% (Fig 6.2). *P. putida* KT2440 have two PHA synthase enzymes ($PhaC1_{Pp}$ and $PhaC2_{Pp}$). Both of them showed high expression level when *P. putida* KT2440 were grown under the conditions for PHA production suggested that $PhaC1_{Pp}$ and $PhaC2_{Pp}$ involved in PHA biosynthesis (62). However, only PhaC1 has been cloned and characterized in recombinant *E. coli* (67, 143). There is no information of heterologous expression of $PhaC2_{Pp}$ in recombinant *E. coli*. Amino acid sequence alignment of $PhaC1_{Pp}$ and $PhaC2_{Pp}$ showed that their identity was 54% (Fig 6.3). On the other hand, three different PhaJ enzymes ($PhaJ1_{Pp}$, $PhaJ4_{Pp}$, and $PhaJ_{Ah}$) which have broad substrate specificity were selected. $PhaJ1_{Pp}$ and $PhaJ4_{Pp}$ were from *P. putida* KT2440 which were identified by homology search of PhaJ1-4 from *P. aeruginosa* against DNA genome sequence of *P. putida* KT2440 (69), whereas $PhaJ_{Ah}$ from *A. hydrophila* (ATCC 7966) has not been characterized previously. Clustal Omega alignment showed that $PhaJ1_{Pp}$, $PhaJ4_{Pp}$, and $PhaJ_{Ah}$ have 26-36% identity of their amino acid sequences (Fig 6.4). The residues forming a catalytic dyad were aspartate and histidine identified based on the crystal structure of *A. caviae* (144). Amino acid sequence of $PhaJ_{Ah}$ was compared with that of PhaJ from *A. caviae* which is well characterized and they showed identity as high as 81% (Fig 6.5).

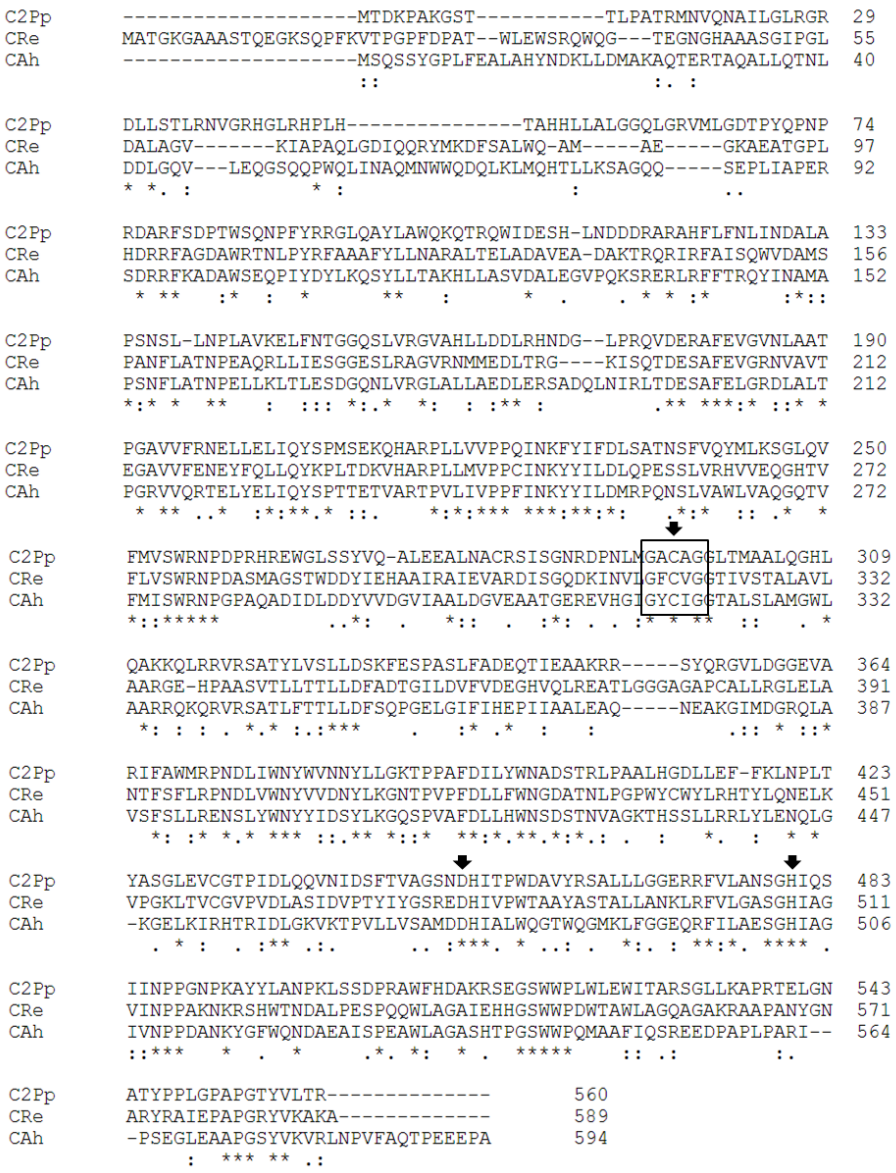

Figure 6.1 Amino acid sequence alignment of PhaCs.

PhaC$_{Ah}$ (CAh), PhaC$_{Re}$ (CRe), and PhaC2$_{Pp}$ (C2Pp) have 594, 589, and 560 amino acids, respectively. The gene IDs of PhaC$_{Ah}$, PhaC$_{Re}$, and PhaC2$_{Pp}$ are 4488480, 4250156, and 1041897, respectively. Their sequences were aligned using Clustal Omega (www.ebi.ac.uk/Tools/msa/clustalo/). They share 36-40% identity. The box indicates the putative lipase box. The arrows indicate the conserved residues involved in catalysis (4). A colon (:) indicates conservation between groups of strongly similar properties. A dot (.) indicates conservation between groups of weakly similar properties. An asterisk (*) indicates identical residues. Numbers indicate the position of amino acids in the respective proteins.

```
CAh      MSQSSYGPLFEALAHYNDKLLDMAKAQTERTAQALLQTNLDDLGQVLEQGSQQPWQLINA   60
CAc      MSQPSYGPLFEALAHYNDKLLAMAKAQTERTAQALLQTNLDDLGQVLEQGSQQPWQLIQA   60
         *** ***************** ************************************:*

CAh      QMNWWQDQLKLMQHTLLKSAGQQSEPLIAPERSDRRFKADAWSEQPIYDYLKQSYLLTAK   120
CAc      QMNWWQDQLKLMQHTLLKSAGQPSEPVITPERSDRRFKAEAWSEQPIYDYLKQSYLLTAR   120
         ********************** ***:*:**********:******************:

CAh      HLLASVDALEGVPQKSRERLRFFTRQYINAMAPSNFLATNPELLKLTLESDGQNLVRGLA   180
CAc      HLLASVDALEGVPQKSRERLRFFTRQYVNAMAPSNFLATNPELLKLTLESDGQNLVRGLA   180
         ***************************:********************************

CAh      LLAEDLERSADQLNIRLTDESAFELGRDLALTPGRVVQRTELYELIQYSPTTETVARTPV   240
CAc      LLAEDLERSADQLNIRLTDESAFELGRDLALTPGRVVQRTELYELIQYSPTTETVGKTPV   240
         ************************************************************.:***

CAh      LIVPPFINKYYILDMRPQNSLVAWLVAQGQTVFMISWRNPGPAQADIDLDDYVVDGVIAA   300
CAc      LIVPPFINKYYIMDMRPQNSLVAWLVAQGQTVFMISWRNPGVAQAQIDLDDYVVDGVIAA   300
         ************:*************************** ***:**************

CAh      LDGVEAATGEREVHGIGYCIGGTALSLAMGWLAARRQKQRVRSATLFTTLLDFSQPGELG   360
CAc      LDGVEAATGEREVHGIGYCIGGTALSLAMGWLAARRQKQRVRTATLFTTLLDFSQPGELG   360
         ******************************************:*****************

CAh      IFIHEPIIAALEAQNEAKGIMDGRQLAVSFSLLRENSLYWNYYIDSYLKGQSPVAFDLLH   420
CAc      IFIHEPIIAALEAQNEAKGIMDGRQLAVSFSLLRENSLYWNYYIDSYLKGQSPVAFDLLH   420
         ************************************************************

CAh      WNSDSTNVAGKTHSSLLRRLYLENQLGKGELKIRHTRIDLGKVKTPVLLVSAMDDHIALW   480
CAc      WNSDSTNVAGKTHNSLLRRLYLENQLVKGELKIRNTRIDLGKVKTPVLLVSAVDDHIALW   480
         *************.************ *******.*****************:*******

CAh      QGTWQGMKLFGGEQRFILAESGHIAGIVNPPDANKYGFWQNDAEAISPEAWLAGASHTPG   540
CAc      QGTWQGMKLFGGEQRFLLAESGHIAGIINPPAANKYGFWHNGAEAESPESWLAGATHQGG   540
         ****************:**********:*** *******:* *** ***:*****:*  *

CAh      SWWPQMAAFIQSREEDPAPLPARIPSEGLEAAPGSYVKVRLNPVFAQTPEEEPA 594
CAc      SWWPEMMGFIQNRDEGSEPVPARVPEEGLAPAPGHYVKVRLNPVFACPTEEDAA 594
         ****:* .***.*:*   *:***:*.***  *** ***********   **: *
```

Figure 6.2 Amino acid sequence alignment of PhaC from *A. hydrophila* ATCC 7966 and from *A. caviae*.

Both $PhaC_{Ah}$ from *A. hydrophila* ATCC 7966 (CAh) and $PhaC_{Ac}$ from *A. caviae* (CAc) have 594 amino acids. The sequence IDs of $PhaC_{Ah}$ and $PhaC_{Ac}$ are 4488480 and 325300783, respectively. Their sequences were aligned using Clustal Omega (www.ebi.ac.uk/Tools/msa/clustalo/). They share 92% identity. A colon (:) indicates conservation between groups of strongly similar properties. A dot (.) indicates conservation between groups of weakly similar properties. An asterisk (*) indicates identical residues. Numbers indicate the position of amino acids in the respective proteins.

```
C1Pp      MSNKNNDELQRQASENTLGLNPVIGIRRKDLLSSARTVLRQAVRQPLHSAKHVAHFGLEL  60
C2Pp      MTDKPAKGSTTLPATRMNVQNAILGLRGRDLLSTLRNVGRHGLRHPLHTAHHLLALGGQL  60
          *::*  .      : .    * ::*:* :****: *.* *:.:*:***:*:*:  :* :*

C1Pp      KNVLLGKSSLAPDSDDRRFNDPAWSNNPLYRRYLQTYLAWRKELQDWVSSSDLSPQDISR  120
C2Pp      GRVMLGDTPYQPNPRDARFSDPTWSQNPFYRRGLQAYLAWQKQTRQWIDESHLNDDDRAR  120
           .*:**.:   *:  * **.**:**:**:*** **:****:*: ::*:..*.*. :* :*

C1Pp      GQFVINLMTEAMAPTNTLSNPAAVKRFFETGGKSLLDGLSNLAKDMVNNGGMPSQVNMDA  180
C2Pp      AHFLFNLINDALAPSNSLLNPLAVKELFNTGGQSLVRGVAHLLDDLRHNDGLPRQVDERA  180
          .:*::**:.:*:**:*:* ** ***.:*:***:**: *::.* .*: .* *:* **:  *

C1Pp      FEVGKNLGTSEGAVVYRNDVLELIQYSPITEQVHARPLLVVPPQINKFYVFDLSPEKSLA  240
C2Pp      FEVGVNLAATPGAVVFRNELLELIQYSPMSEKQHARPLLVVPPQINKFYIFDLSATNSFV  240
          **** **.:: ****:**::********::*: ****************:****  :*:.

C1Pp      RFCLRSQQQTFIISWRNPTKAQREWGLSTYIDALKEAVDAVLSITGSKDLNMLGACSGGI  300
C2Pp      QYMLKSGLQVFMVSWRNPDPRHREWGLSSYVQALEEALNACRSISGNRDPNLMGACAGGL  300
          :: *:*  *.*::*****   :******:*::**:**::*  **:*.:* *::***:**:

C1Pp      TCTALVGHYAAIGE-NKVNALTLLVSVLDTTMDNQVALFVDEQTLEAAKRHSYQAGVLEG  359
C2Pp      TMAALQGHLQAKKQLRRVRSATYLVSLLDSKFESPASLFADEQTIEAAKRRSYQRGVLDG  360
          * :** **  *  : .:*.: * ***:**:.::. .:**.****:*****:*** ***:*

C1Pp      SEMAKVFAWMRPNDLIWNYWVNNYLLGNEPPVFDILFWNNDTTRLPAAFHGDLIEMFKSN  419
C2Pp      GEVARIFAWMRPNDLIWNYWVNNYLLGKTPPAFDILYWNADSTRLPAALHGDLLEFFKLN  420
          .*:*::********************: **.****:** *:******:****:*:** *

C1Pp      PLTRPDALEVCGTAIDLKQVKCDIYSLAGTNDHITPWPSCYRSAHLFGGKIEFVLSNSGH  479
C2Pp      PLTYASGLEVCGTPIDLQQVNIDSFTVAGSNDHITPWDAVYRSALLLGGERRFVLANSGH  480
          ***  ..****** ***:**: * :::**:******* : **** *:**: .***:****

C1Pp      IQSILNPPGNPKARFMTGADRPGDPVAWQENAIKHADSWWLHWQSWLGERAGALKKAPTR  539
C2Pp      IQSIINPPGNPKAYYLANPKLSSDPRAWFHDAKRSEGSWWPLWLEWITARSGLLKAPRTE  540
          ****:******** :::  .  .** ** .:* :   ***  * .*:  *:* **   *.

C1Pp      LGNRTYAAGEASPGTYVHER  559
C2Pp      LGNATYPPLGPAPGTYVLTR  560
          *** **     :*****  *
```

Figure 6.3 Amino acid sequence alignment of PhaC1 and PhaC2 from *P. putida* KT2440.

PhaC1$_{Pp}$ (C1Pp) and PhaC2$_{Pp}$ (C2Pp) have 559 and 560 amino acids, respectively. The gene IDs of PhaC1$_{Pp}$ and PhaC2$_{Pp}$ are 1041855 and 1041897, respectively. Their sequences were aligned using Clustal Omega (www.ebi.ac.uk/Tools/msa/clustalo/). They share 54% identity. A colon (:) indicates conservation between groups of strongly similar properties. A dot (.) indicates conservation between groups of weakly similar properties. An asterisk (*) indicates identical residues. Numbers indicate the position of amino acids in the respective proteins.

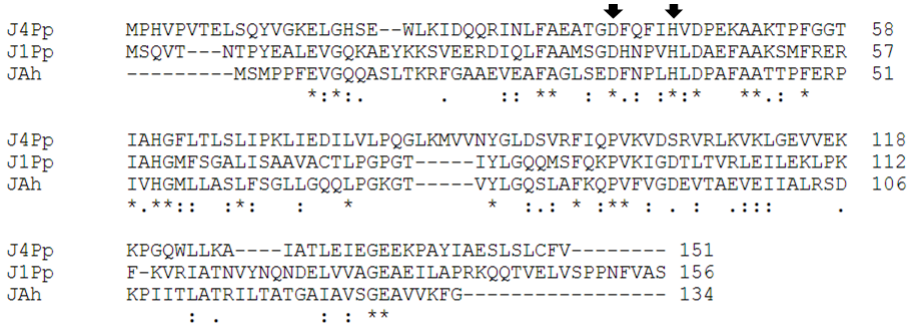

Figure 6.4 Amino acid sequence alignment of PhaJs.

PhaJ$_{Ah}$ (JAh), PhaJ1$_{Pp}$ (J1Pp), and PhaJ4$_{Pp}$ (J4Pp) have 134, 156, and 151 amino acids. The gene IDs of PhaJ$_{Ah}$, PhaJ1$_{Pp}$ and PhaJ$_{4Pp}$ are 1046178, 1045908, and 4488481, respectively. Their sequences were aligned using Clustal Omega (www.ebi.ac.uk/Tools/msa/clustalo/). They share 26-36% identity. The arrows indicate the conserved residues involved in catalysis (12)**.** A colon (:) indicates conservation between groups of strongly similar properties. A dot (.) indicates conservation between groups of weakly similar properties. An asterisk (*) indicates identical residues. Numbers indicate the position of amino acids in the respective proteins.

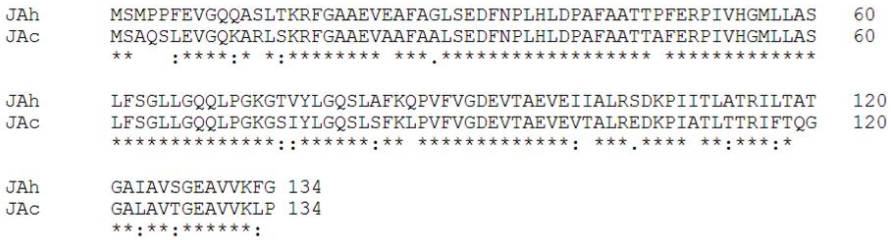

Figure 6.5 Amino acid sequence alignment of PhaJ from *A. hydrophila* ATCC 7966 and from *A. caviae*.

Both PhaJ$_{Ah}$ (JAh) and PhaJ$_{Ac}$ (JAc) have 134 amino acids. The sequence IDs of PhaJ$_{Ah}$ and PhaJ$_{Ac}$ are 4488481 and 2335048, respectively. Their sequences were aligned using Clustal Omega (www.ebi.ac.uk/Tools/msa/clustalo/). They share 81% identity. A colon (:) indicates conservation between groups of strongly similar properties. A dot (.) indicates conservation between groups of weakly similar properties. An asterisk (*) indicates identical residues. Numbers indicate the position of amino acids in the respective proteins.

6.1.2 Plasmid construction

To establish the PHA biosynthetic pathway, two sets of recombinant plasmids were constructed. The first one was pETDuet-1 vector harboring *phaA*, *phaB*, and *phaC*. The second one was pCDFDuet-1 vector harboring *phaJ*. As three types of phaC and three types of phaJ were used, six resulting recombinant plasmids namely pETDuet-ABC_{Re}, pETDuet-ABC_{Ah}, pETDuet-$ABC2_{Pp}$, pCDFDuet-$J1_{Pp}$, pCDFDuet-$J4_{Pp}$, and pCDFDuet-J_{Ah} were constructed (Fig 5.2). All genes were PCR amplified from the genomic DNA of native PHA producing strains. The thick bands of extracted genomic DNA are found at the position higher than 23 kb (Fig 6.6). The PCR amplified fragments were purified by excising only the target PCR bands of $phaAB_{Re}$, $phaC_{Re}$, $phaC_{Ah}$, and $phaC2_{Pp}$ (Fig 6.7). The PCR amplified fragment of $phaJ1_{Pp}$, $phaJ4_{Pp}$, and $phaJ_{Ah}$ are shown in Figure 6.8.

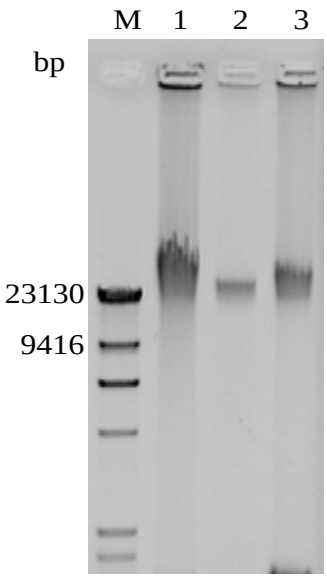

Figure 6.6 Genomic DNA extracted from wild type PHA-producing bacteria.

Agarose gel electrophoresis of genomic DNA from wild type PHA-producing bacteria using SDS-based DNA extraction method with ethylenediaminetetraacetic acid (EDTA) and phenol chloroform. Lane M is λ/*Hind*III marker. Lanes 1-3 are extracted genomic DNA from *R. eutropha*, *A. hydrophila*, and *P. putida* respectively.

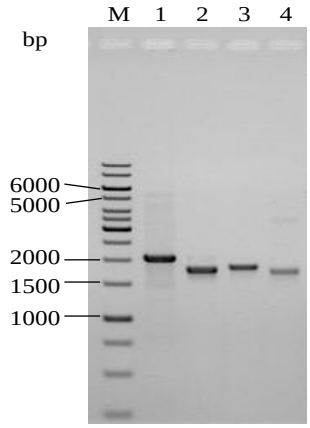

Figure 6.7 PCR amplification of β-ketothiolase (*phaA*), NADPH-dependent acetoacetyl-CoA reductase (*phaB*), and PHA synthase (*phaC*) genes from genomic DNA of wild type PHA-producing bacteria.

Agarose gel electrophoresis of the DNA fragment from PCR amplification of *phaA, phaB,* and *phaC* purified genomic DNA. Lane M is 1 kb DNA marker. Lane 1, *phaA-phaB* from *R. eutropha* (the expected size is ~2.0 kb); lane 2, *phaC* of *R. eutropha* (the expected size is ~1.8 kb); lane 3, *phaC* of *A. hydrophila* (the expected size is ~1.8 kb); lane 4, *phaC*2 of *P. putida* (the expected size is ~1.7 kb).

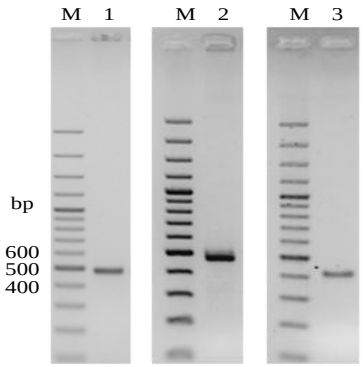

Figure 6.8 PCR amplification of (*R*)-specific enoyl-CoA hydratase (*phaJ*) genes from genomic DNA of wild type PHA-producing bacteria.

Agarose gel electrophoresis of the DNA fragment from PCR amplification. Lane M is 100 bp DNA ladder plus marker. Lane 1, *phaJ*1 from *P. putida* (the expected PCR fragment is 0.48 kb); lane 2, *phaJ*4 from *P. putida* (the expected PCR fragment is 0.46 kb); lane 3, *phaJ* from *A. hydrophila* (the expected PCR fragment is approximately 0.4 kb).

6.1.3 Protein expression

E. coli BL21(DE3) was used as a host for protein expression and PHA production. Three recombinant *E. coli* strains harboring *phaA, phaB,* and *phaC* namely *E.coli*-AB$_{Re}$C$_{Re}$, *E.coli*-AB$_{Re}$C$_{Ah}$, *and E.coli*-AB$_{Re}$C2$_{Pp}$ were tested for their ability to co-express PhaABC in LB medium. The heterologous protein expression of β-ketothiolase (PhaA), NADPH-dependent acetoacetyl-CoA reductase (PhaB), and PHA synthase (PhaC) proteins in *E. coli* BL21(DE3) is shown (Fig 6.9). The results showed that all target recombinant proteins were expressed under the condition used. Compared to the *E. coli* strain harboring the empty vector pETDuet-1, PhaA$_{Re}$, PhaC$_{Re}$, PhaC$_{Ah}$, and PhaC2$_{Pp}$ were clearly expressed from the recombinants. However, the expression level of each protein was different. From SDS-PAGE analysis, the expression of PhaB$_{Re}$ was not clear but its expression was confirmed by western blot (Fig 6.9B). The expression of PhaJ in *E. coli*-J1$_{Pp}$, *E. coli*-J4$_{Pp}$, and *E. coli*-J$_{Ah}$ were verified. SDS-PAGE and western blot analysis using anti-His$_6$ showed that all three PhaJs were expressed (Fig 6.10). Although the expression of PhaJ4$_{Pp}$ and PhaJ$_{Ah}$ could not be clearly seen from SDS-PAGE, they were detectable using western blot.

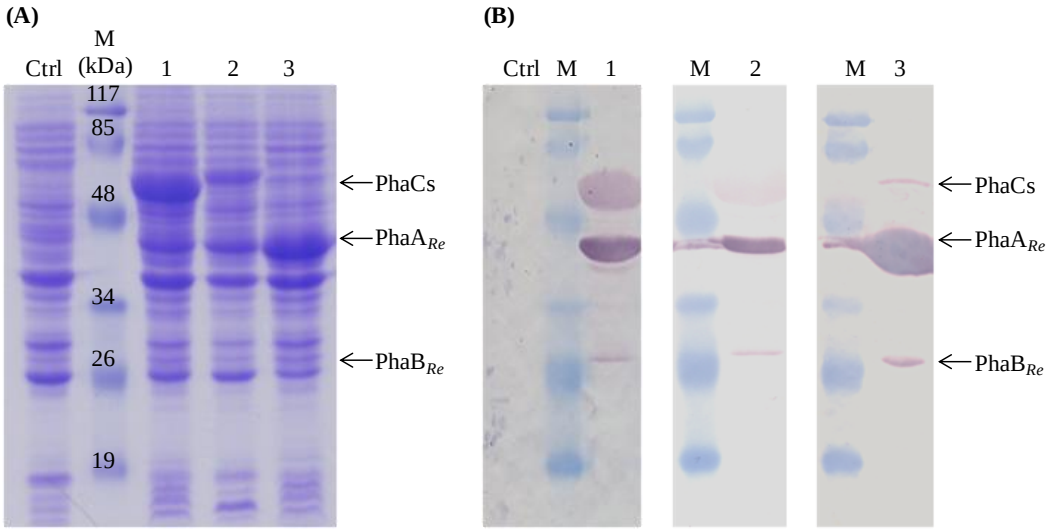

Figure 6.9 Heterologous protein expression of β-ketothiolase (PhaA), NADPH-dependent acetoacetyl-CoA reductase (PhaB), and PHA synthase (PhaC) proteins in *E. coli* BL21(DE3).

(A) SDS-PAGE analysis of protein profiles of *E. coli*-ABC$_{Re}$, *E. coli*-ABC$_{Ah}$, and *E. coli*-ABC2$_{Pp}$ cultured in LB medium and induced with 1 mM IPTG for 3 h. (B) western blot analysis using anti-polyHistidine monoclonal antibody. Lane M is Prestained Protein molecular weight marker. Lanes 1-3 are the proteins from *E. coli*-ABC$_{Re}$, *E. coli*-ABC$_{Ah}$, and *E. coli*-ABC2$_{Pp}$, respectively. Ctrl is proteins from *E. coli*-pETDuet-1 (control). The expected size of PhaA$_{Re}$, PhaB$_{Re}$, PhaC$_{Re}$, PhaC$_{Ah}$, and PhaC2$_{Pp}$ are 42 kDa, 27 kDa, 66 kDa, 68 kDa, and 64 kDa, respectively. Arrows indicate the expressed recombinant proteins. The samples were loaded at equivalent OD_{600}.

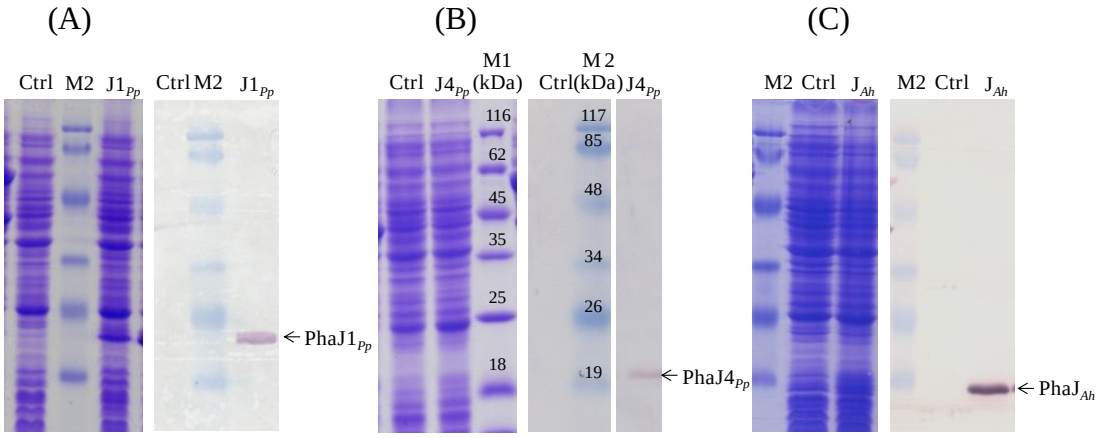

Figure 6.10 SDS-PAGE and western blot analysis of heterologous protein expression of (*R*)-specific enoyl-CoA hydratase (PhaJ) proteins in *E. coli* BL21(DE3).

(A) is *E. coli*-J1$_{Pp}$, (B) is *E. coli*-J4$_{Pp}$ and (C) is *E. coli*-J$_{Ah}$. Cells were cultured in LB medium and induced with 1 mM IPTG for 3 h. Western blot analysis was performed using anti-polyHistidine monoclonal antibody. Lanes M1 and M2 are Unstained and Prestained Protein molecular weight marker. Ctrl is proteins from *E. coli*-PCDFDuet-1 (control). PhaJ1$_{Pp}$, PhaJ4$_{Pp}$, and PhaJ$_{Ah}$ proteins are indicated by arrows. The predicted protein molecular weight of PhaJ1$_{Pp}$, PhaJ4$_{Pp}$, and PhaJ$_{Ah}$ were 19 kDa, 18 kDa and 16 kDa, respectively. Arrows indicate the expressed recombinant proteins. The samples were loaded at equivalent OD_{600}.

To establish the hybrid pathway for biosynthesis of SCL-MCL-PHAs in *E. coli*, the recombinant plasmids, pETDuet-*ABC*s and pCDFDuet-*J*s, were co-transformed into *E. coli* BL21(DE3). Nine recombinant strains namely, *E. coli*-ABC$_{Re}$J1$_{Pp}$, *E. coli*-ABC$_{Re}$J4$_{Pp}$, *E. coli*-ABC$_{Re}$J$_{Ah}$, *E. coli*-ABC$_{Ah}$J1$_{Pp}$, *E. coli*-ABC$_{Ah}$J4$_{Pp}$, *E. coli*-ABC$_{Ah}$J$_{Ah}$, *E. coli*-ABC2$_{Pp}$J1$_{Pp}$, *E. coli*-ABC2$_{Pp}$J4$_{Pp}$, and *E. coli*-ABC2$_{Pp}$J$_{Ah}$ were generated. Co-expression of PhaA, PhaB, PhaC and PhaJ was verified. Figure 6.11 showed SDS-PAGE and western blot analysis of proteins in recombinant *E. coli*-ABC$_{Re}$J1$_{Pp}$, *E. coli*-ABC$_{Ah}$J1$_{Pp}$, and *E. coli*-ABC2$_{Pp}$J1$_{Pp}$. Figure 6.12 showed SDS-PAGE and western blot analysis of proteins in recombinant *E. coli*-ABC$_{Re}$J4$_{Pp}$, *E. coli*-ABC$_{Ah}$J4$_{Pp}$, and *E. coli*-ABC2$_{Pp}$J4$_{Pp}$. Figure 6.13 showed SDS-PAGE and western blot analysis of proteins in recombinant *E. coli*-ABC$_{Re}$J$_{Ah}$, *E. coli*-ABC$_{Ah}$J$_{Ah}$, and *E. coli*-ABC2$_{Pp}$J$_{Ah}$. The results showed that all recombinant proteins were co-expressed in *E. coli*.

(A)

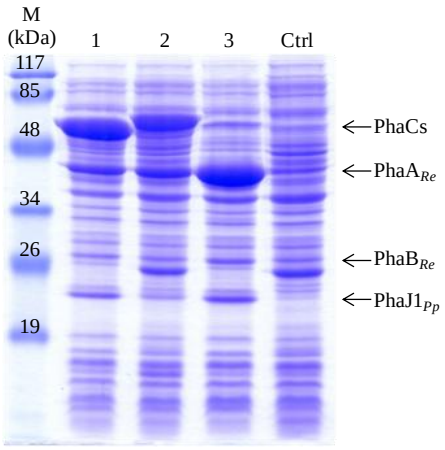

(B)

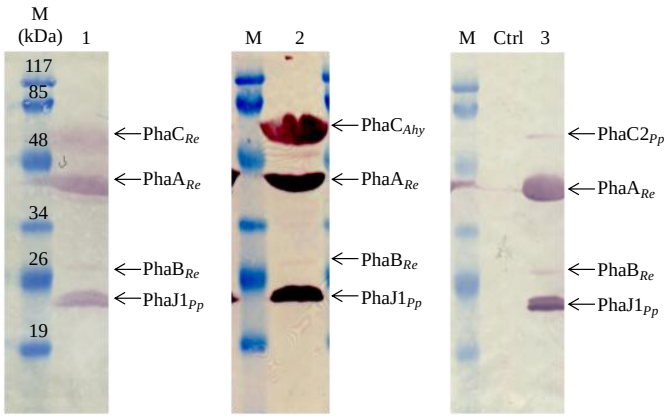

Figure 6.11 Co-expression of β-ketothiolase (PhaA), NADPH-dependent acetoacetyl-CoA reductase (PhaB), PHA synthase (PhaC) and (*R*)-specific enoyl-CoA hydratase (PhaJ1$_{Pp}$) proteins in *E. coli* BL21(DE3).

(A) SDS-PAGE analysis of protein profiles of *E. coli*-ABC$_{Re}$J1$_{Pp}$, *E. coli*-ABC$_{Ah}$J1$_{Pp}$, and *E. coli*-ABC2$_{Pp}$J1$_{Pp}$ cultured in LB medium and induced with 1 mM IPTG for 3 h. (B) Western blot analysis using anti-polyHistidine monoclonal antibody. Lane M is Prestained Protein molecular weight marker. Lanes 1-3 are the proteins from *E. coli*-ABC$_{Re}$J1$_{Pp}$, *E. coli*-ABC$_{Ah}$J1$_{Pp}$, and *E. coli*-ABC2$_{Pp}$J1$_{Pp}$, respectively. Ctrl is proteins from *E. coli*-pETDuet-1+pCDFDuet-1 (control). The expected size of PhaA$_{Re}$, PhaB$_{Re}$, PhaC$_{Re}$, PhaC$_{Ah}$, PhaC2$_{Pp}$ and PhaJ1$_{Pp}$ are 42 kDa, 27 kDa, 66 kDa, 68 kDa, 64 kDa, and 19 kDa, respectively. Arrows indicate the expressed recombinant proteins. The samples were loaded at equivalent OD_{600}.

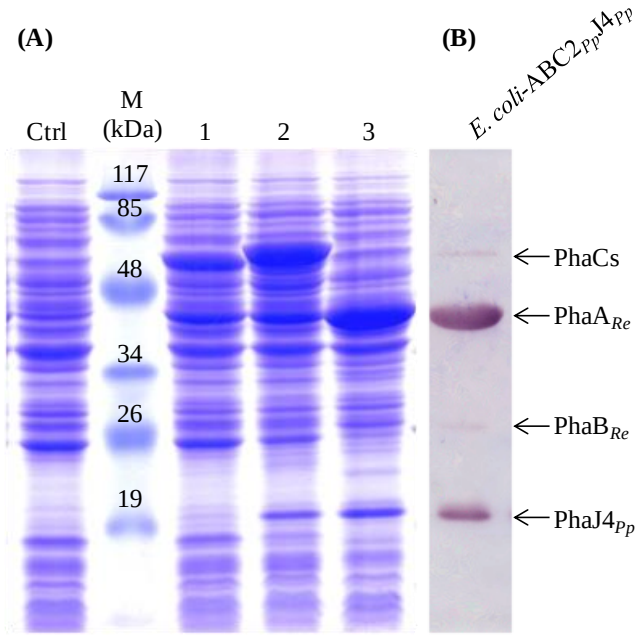

Figure 6.12 Co-expression of β-ketothiolase (PhaA), NADPH-dependent acetoacetyl-CoA reductase (PhaB), PHA synthase (PhaC) and (*R*)-specific enoyl-CoA hydratase (PhaJ4$_{Pp}$) proteins in *E. coli* BL21(DE3).

(A) SDS-PAGE analysis of protein profiles of *E. coli*-ABC$_{Re}$J4$_{Pp}$, *E. coli*-ABC$_{Ah}$J4$_{Pp}$, and *E. coli*-ABC2$_{Pp}$J4$_{Pp}$ cultured in LB medium and induced with 1 mM IPTG for 3 h. (B) western blot analysis using anti-polyHistidine monoclonal antibody. Lane M is Prestained Protein molecular weight marker. Lanes 1-3 are the proteins from *E. coli*-ABC$_{Re}$J4$_{Pp}$, *E. coli*-ABC$_{Ah}$J4$_{Pp}$, and *E. coli*-ABC2$_{Pp}$J4$_{Pp}$ respectively. Ctrl is proteins from *E. coli*-pETDuet-1+pCDFDuet-1 (control). The expected size of PhaA$_{Re}$, PhaB$_{Re}$, PhaC$_{Re}$, PhaC$_{Ah}$, PhaC2$_{Pp}$ and PhaJ4$_{Pp}$ are 42 kDa, 27 kDa, 66 kDa, 68 kDa, 64 kDa, and 18 kDa, respectively. Arrows indicate the expressed recombinant proteins. The samples were loaded at equivalent OD_{600}.

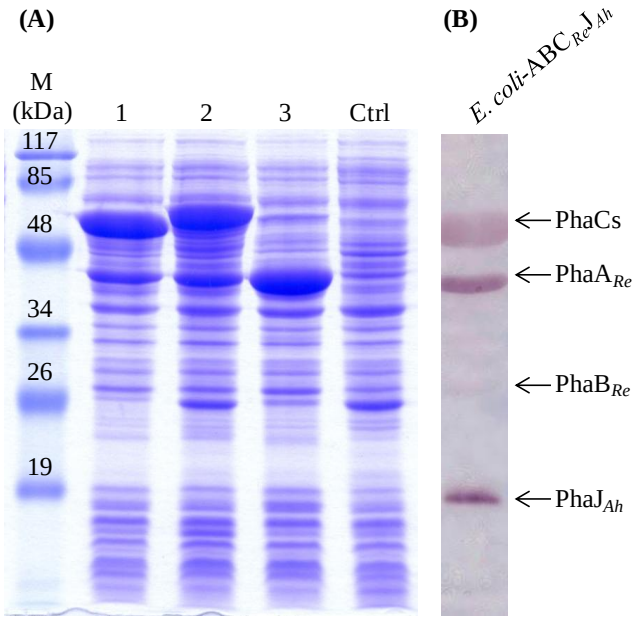

Figure 6.13 Co-expression of β-ketothiolase (PhaA), NADPH-dependent acetoacetyl-CoA reductase (PhaB), PHA synthase (PhaC) and (*R*)-specific enoyl-CoA hydratase (PhaJ$_{Ah}$) proteins in *E. coli* BL21(DE3).

(A) SDS-PAGE analysis of protein profiles of *E. coli*-ABC$_{Re}$J$_{Ah}$, *E. coli*-ABC$_{Ah}$J$_{Ah}$, and *E. coli*-ABC2$_{Pp}$J$_{Ah}$ cultured in LB medium and induced with 1 mM IPTG for 3 h. (B) Western blot analysis using anti-polyHistidine monoclonal antibody. Lane M is Prestained Protein molecular weight marker. Lanes 1-3 are the proteins from *E. coli*-ABC$_{Re}$J$_{Ah}$, *E. coli*-ABC$_{Ah}$J$_{Ah}$, and *E. coli*-ABC2$_{Pp}$J$_{Ah}$ respectively. Ctrl is proteins from *E. coli*-pETDuet-1+pCDFDuet-1 (control). The expected size of PhaA$_{Re}$, PhaB$_{Re}$, PhaC$_{Re}$, PhaC$_{Ah}$, PhaC2$_{Pp}$ and PhaJ$_{Ah}$ are 42 kDa, 27 kDa, 66 kDa, 68 kDa, 64 kDa, and 16 kDa, respectively. Arrows indicate the expressed recombinant proteins. The samples were loaded at equivalent OD_{600}.

6.2 Using pure glycerol as a carbon source for PHAs biosynthesis

6.2.1 P(3HB) biosynthesis

6.2.1.1 Effect of different PhaC types on growth and P(3HB) biosynthesis by *E. coli*-ABCs

The ability of recombinant *E. coli* harboring PhaA, PhaB, and PhaCs (*E. coli*-ABC$_{Re}$, *E. coli*-ABC$_{Ah}$, and *E. coli*-ABC2$_{Pp}$) to synthesize P(3HB) by using pure glycerol as the sole carbon source was investigated by cultivating the recombinant strains in M9 medium containing glycerol. Their growth curve profiles were determined (Fig 6.14). All strains reached the log phase and stationary phase at 3 h and 15 h after inoculation, respectively. IPTG (1mM) was added to the culture media for induction of recombinant proteins at 6 h after inoculation (early log phase). The expression of recombinant proteins from each recombinant strains are shown (Fig 6.15). Accumulation of P(3HB) granules inside the cells were detected by Nile Blue A staining analysis. The stained cells were observed under Fluorescence Microscope Olympus (UIS Fluorescence) at 400x (Fig 6.16). The result showed that *E. coli*-ABC$_{Re}$ and *E. coli*-ABC$_{Ah}$ emitted orange fluorescence whereas *E. coli*-ABC2$_{Pp}$ did not emit orange fluorescence suggesting that *E. coli*-ABC$_{Re}$ and *E. coli*-ABC$_{Ah}$ can accumulate P(3HB) granules inside the cells under conditions used. Moreover, the round orange granules of P(3HB) accumulated inside of *E. coli*-ABC$_{Re}$ and *E. coli*-ABC$_{Ah}$ were clearly shown by observing under Confocal Laser Scanning Microscope model Olympus FV1000 at 1000x (Fig 6.17). To quantitate the P(3HB) content, the dried cells of each recombinant were digested by H_2SO_4 to its derivative monomer and subjected to HPLC analysis. The results showed that different sources of PhaC gave different level of P(3HB) (Table 6.1). *E. coli*-ABC$_{Ah}$, *E. coli*-ABC$_{Re}$, and *E. coli*-ABC2$_{Pp}$ accumulated P(3HB) at 30 wt%, 24 wt% and 2 wt% content of dry cell weight, respectively. Since *E. coli*-ABC$_{Ah}$ was able to produce the highest amount of P(3HB), therefore this recombinant strain was then used for further investigating the effect of some cultivation parameters on the production of P(3HB).

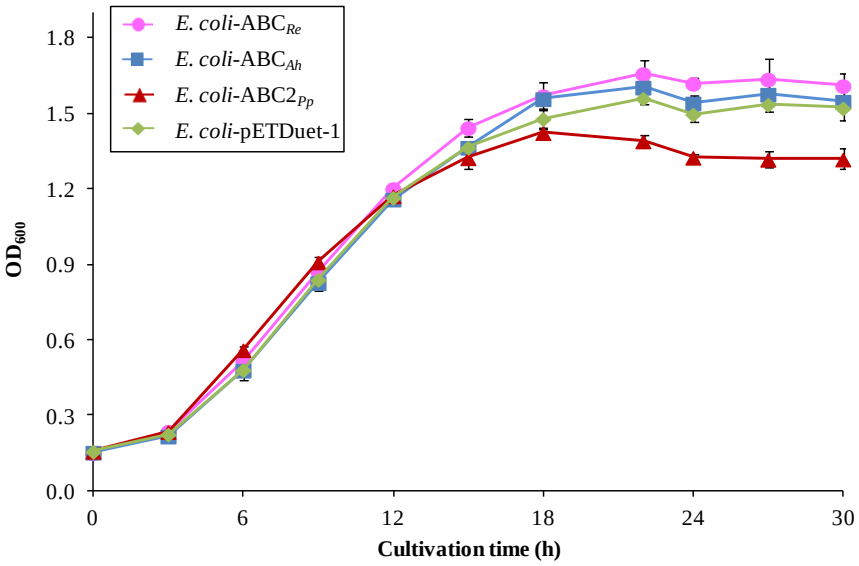

Figure 6.14 Growth profiles of recombinant *E. coli*-ABCs strains cultured in minimum medium (M9) containing 2% (v/v) glycerol as a sole carbon source. Result is the average value and error bar represents standard deviation for triplicate experiments.

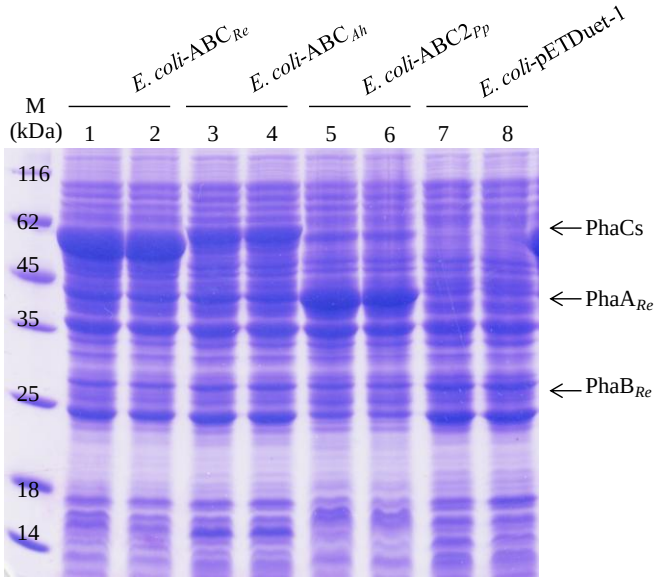

Figure 6.15 Protein expression profiles of *E. coli*-ABC$_{Re}$, *E. coli*-ABC$_{Ah}$, and *E. coli*-ABC2$_{Pp}$ analyzed by SDS-PAGE.

SDS-PAGE analysis of protein profiles of *E. coli*-ABC$_{Re}$, *E. coli*-ABC$_{Ah}$, and *E. coli*-ABC2$_{Pp}$ cultured in M9 medium containing 2% (v/v) glycerol as a sole carbon source. The cells were induced with 1 mM IPTG after 6 h inoculation and harvested after 24 h. Lane M is Unstained Protein molecular weight marker. Lanes 1-2, 3-4, 5-6, and 7-8 are the proteins from *E. coli*-ABC$_{Re}$, *E. coli*-ABC$_{Ah}$, *E. coli*-ABC2$_{Pp}$, and *E. coli*-pETDuet-1, respectively. The expected size of PhaA$_{Re}$, PhaB$_{Re}$, PhaC$_{Re}$, PhaC$_{Ah}$, and PhaC2$_{Pp}$ are 42 kDa, 27 kDa, 66 kDa, 68 kDa, and 64 kDa, respectively. Arrows indicate the expressed recombinant proteins. The samples were loaded at equivalent OD_{600}.

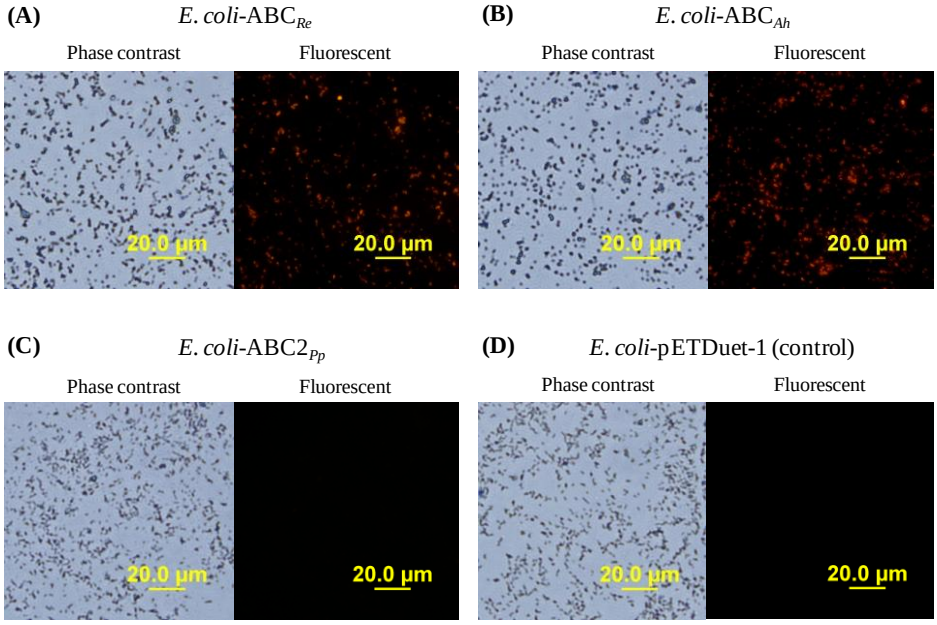

Figure 6.16 Nile blue A fluorescent dye staining of P(3HB) granules in recombinant *E. coli*-ABCs.

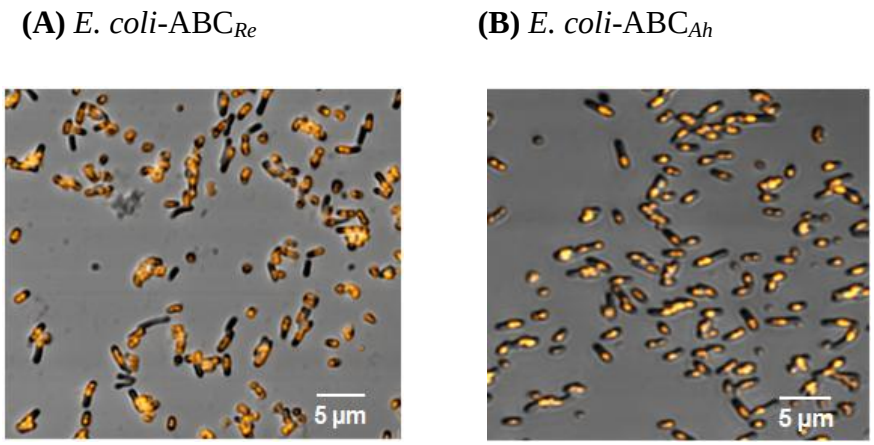

Figure 6.17 Nile blue A fluorescent dye staining of P(3HB) granules in recombinant *E. coli*-ABCs as observed by confocal laser scanning microscope.

(A) *E. coli*-ABC$_{Re}$, (B) *E. coli*-ABC$_{Ah}$, (C) *E. coli*-ABC2$_{Pp}$, and (D) *E. coli*-pETDuet-1 (control). The recombinant *E. coli* were cultured in M9 containing 2% (v/v) glycerol as sole carbon source and induced with 1 mM IPTG for 24 hr. The micrographs were taken under Fluorescence Microscope Olympus (UIS Fluorescence) at 400x (Fig 6.16) and under Confocal Laser Scanning Microscope model Olympus FV1000 at 1000x (Fig 6.17).

Table 6.1 P(3HB) biosynthesis in recombinant *E. coli* harboring *phaABC*s [reproduced from (19) with permission from JSBA]**.**

Strains	CDW (g/L)	P(3HB) content (wt% of CDW)	P(3HB) (mg/L)
E. coli-ABC$_{Ah}$	1.23 ± 0.05	30.4 ± 1.61	371.8 ± 32.64
E. coli-ABC$_{Re}$	1.08 ± 0.05	24.4 ± 0.95	264.9 ± 21.16
E. coli-ABC2$_{Pp}$	0.95 ± 0.01	1.8 ± 0.23	13.5 ± 2.37
E. coli-pETDuet-1 (control)	0.82 ± 0.003	-	-

Cells were cultivated at 37°C in M9 minimum medium containing 2% (v/v) glycerol as the sole carbon source. After 6 h of cultivation, IPTG (1mM) was added and cells were grown for additional 24 h. Results are the average ± standard deviations from three independent experiments. CDW, cell dry weight; -, not detectable.

6.2.1.2 Effect of glycerol concentration on growth and P(3HB) biosynthesis by *E. coli*-ABC$_{Ah}$

The effect of glycerol concentration on the growth of *E. coli*-ABC$_{Ah}$ was investigated. Glycerol concentrations varying from 1% to 15% (v/v) were used as a carbon source for cultivating *E. coli*-ABC$_{Ah}$. The cultured cells were collected at various intervals to measure the OD_{600} (Fig 6.18). The growth profiles of *E. coli*-ABC$_{Ah}$ cultured in the medium containing 1%, 2%, or 5% (v/v) glycerol were similar, having their maximal OD_{600} over 2.0. But in 10% and 15% (v/v) glycerol, the growths of *E. coli*-ABC$_{Ah}$ were slower and their maximum OD_{600} were around 1.5. Therefore, glycerol concentrations up to only 5% (v/v) were used as a carbon source to evaluate their effect on the ability to produce P(3HB) of *E. coli*-ABC$_{Ah}$. After 3 h inoculation, the cultured cells were induced by 1 mM IPTG and cultured for further 24 h. Cell dry weight, P(3HB) content, and the remaining glycerol in the supernatant after cell harvested were determined (Table 6.2). The result showed that the maximal cell dry weight and the amount of P(3HB) were obtained from 1% (v/v) glycerol.

However, only a slight decrease of cell dry weight and the amount of P(3HB) were found with increasing glycerol concentration. Moreover, it was found that glycerol still remained in the culture media after cultivation for 27 h in all concentrations used.

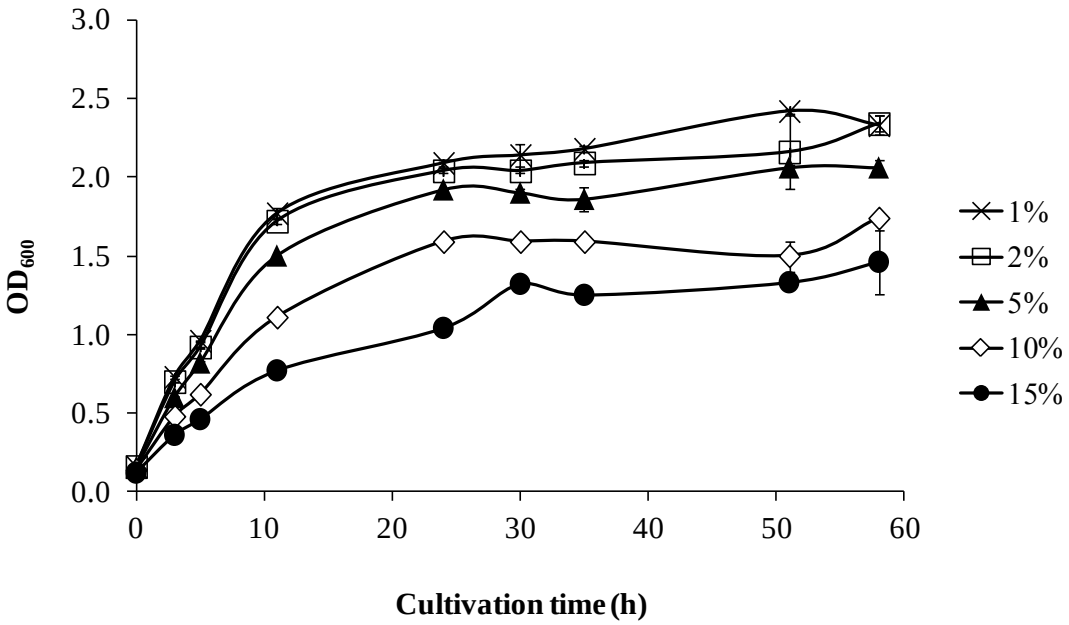

Figure 6.18 Effect of glycerol concentration on the growth profiles of *E. coli*-ABC$_{Ah}$.

E. coli-ABC$_{Ah}$ was cultured in M9 minimum medium supplemented with yeast extract with 1%, 2%, 5%, 10%, and 15% (v/v) glycerol as a carbon source. The cultured cells were collected at 0, 3, 5, 11, 24, 30, 35, 51, and 58 h after inoculation and OD_{600} of the cultured media were measured. Result is the average value and error bar represents standard deviation for triplicate experiment.

Table 6.2 Effect of glycerol concentration on P(3HB) biosynthesis.

Glycerol (% v/v)	CDW (g/L)	P(3HB) content (wt% of CDW)	P(3HB) (g/L)	Remaining glycerol (% v/v)
1	1.6 ± 0.10	23.2 ± 0.92	0.37 ± 0.04	0.2 ± 0.03
2	1.4 ± 0.10	21.7 ± 0.92	0.30 ± 0.01	1.3 ± 0.02
3	1.4 ± 0.10	18.3 ± 1.33	0.25 ± 0.01	2.4 ± 0.06
5	1.3 ± 0.15	19.9 ± 0.56	0.27 ± 0.02	4.3 ± 0.04

Cells were cultivated at 37°C in M9 minimum medium containing glycerol as the sole carbon source supplemented with 1 g/L Bacto-yeast extract. After 3 h of cultivation, IPTG (1mM) was added and cells were grown for an additional 24 h. Results are the average ± standard deviations from triplicate experiment. CDW, cell dry weight.

6.2.1.3 Effect of carbon and nitrogen source on growth and P(3HB) biosynthesis by *E. coli*-ABC$_{Ah}$

P(3HB) production using glycerol as a carbon source was compared to glucose as a sole carbon source. Moreover, the effect of adding yeast extract into the culture media was also evaluated. To investigate the effect of carbon and nitrogen source on the growth of *E. coli*-ABC$_{Ah}$, the cells were cultured in the media containing glycerol or glucose at 2% (w/v) as a carbon source with or without yeast extract. The cultured cells were collected every 3 h until 33 h to measure the OD_{600} and pH. In all culture media, the highest cell density was equal at 30 h. By using glycerol as a carbon source, cells grew slower than that using glucose. When yeast extract was supplemented in the culture media with either glycerol or glucose as a carbon source, cell grew rapidly, had shorter lag phase and entered into the stationary phase within 14 h. Whereas when the cells were grown in the media without yeast extract, they grew slower, with longer lag phase and entered into the stationary phase after 14 h (Fig 6.19). The pH of the culture media decreased rapidly when cells were grown in glucose within 14 h. At 30 h, pH was drop to 5.0 and 4.5 when cells were grown in glycerol and glucose, respectively (Fig 6.20).

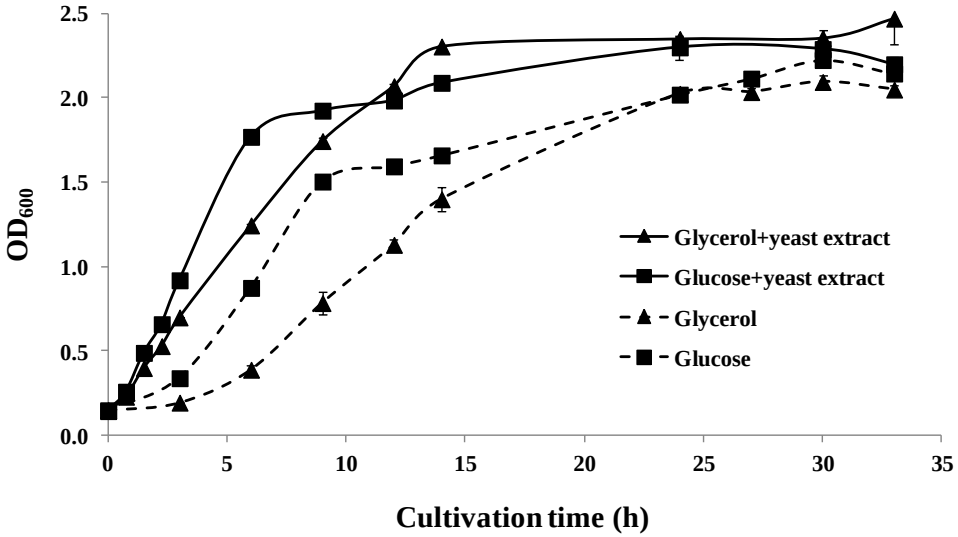

Figure 6.19 Effect of carbon and nitrogen source on the growth profiles of *E. coli*-ABC$_{Ah}$.

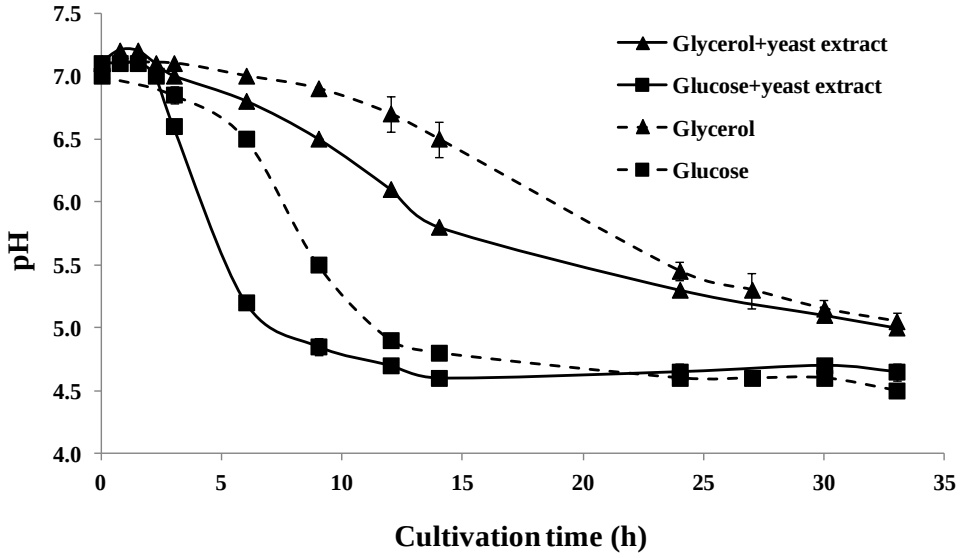

Figure 6.20 Effect of carbon and nitrogen source on pH profiles of *E. coli*-ABC$_{Ah}$.

E. coli-ABC$_{Ah}$ was cultured in four types of media which were M9+glucose+yeast extract, M9+glycerol+yeast extract, M9+glucose, and M9+glycerol. The cultured cells of *E. coli*-ABC$_{Ah}$ were collected at the interval time to measure the OD_{600} and pH. Result is the average value and error bar represents standard deviation for triplicate experiment.

Next, the effect of carbon and nitrogen source on the ability of *E. coli*-ABC$_{Ah}$ to synthesize P(3HB) was investigated. *E. coli*-ABC$_{Ah}$ was cultured in three different media which were M9 medium containing glucose and yeast extract, glycerol and yeast extract, and glycerol only. The cells were induced with 1 mM IPTG at the early log phase. Based on the growth profiles (Fig 6.19), the cells cultured in media with yeast extract were induced at 3 h after inoculation and continued culture for additional 24 h and 48 h. While the cells cultured in media without yeast extract were induced at 6 h after inoculation and continued culture for additional 21 h and 45 h. Therefore, the total cultivation time was the same which were 27 h and 51 h, respectively. % P(3HB) content, P(3HB) (mg/L/h), P(3HB) (g/L), and pH of the culture media were determined (Fig 6.21). By using glycerol as a carbon source, cells produced more P(3HB) when compared to glucose. The productivity of P(3HB) was higher when cells were grown in the media without yeast extract. When the time was increased to 51 h, % P(3HB) content and P(3HB) (g/L) were slightly increased but P(3HB) productivity (mg/L/h) was decreased.

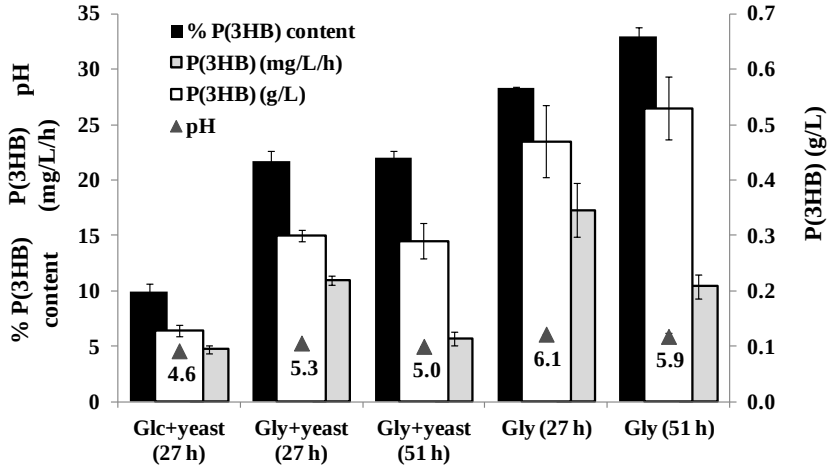

Figure 6.21 Effect of carbon and nitrogen source on the P(3HB) biosynthesis.

E. coli-ABC$_{Ah}$ was cultured in three different media which were M9+glucose+yeast extract, M9+glycerol+yeast extract, and M9+glycerol. The cells were induced with 1 mM IPTG at the early log phase. The cells were harvested at 27 h and 51 h after inoculation to evaluate the P(3HB) content, P(3HB) (mg/L/h), P(3HB) (g/L), and pH. Result is the average value and error bar represents standard deviation for triplicate experiments.

6.2.1.4 Effect of stage of cell at the induction point on P(3HB) biosynthesis

The stage of cell was investigated whether it influences the productivity of P(3HB). *E. coli*-ABC$_{Ah}$ was cultivated in minimum medium containing glycerol as a carbon source. IPTG was added into the culture medium to induce the expression of PhaABC at four different stages of cell: initial inoculation, early log phase, mid log phase, and late log phase. After induction, cells were cultivated for further 24 h and then harvested and the amount of P(3HB) were analyzed by HPLC (Fig 6.22). When induction at early log phase (3 h after inoculation), % P(3HB) content, P(3HB) (mg/L), and the productivity (mg/L/h) were 23 wt% of CDW, 0.4 mg/L, and 13.1 mg/L/h, respectively. These values were the highest when compared to induction at the other cell stages. The induction at the initial and mid log phase gave similar P(3HB) production. The ability for P(3HB) production was the lowest when the cells were induced at late log phase.

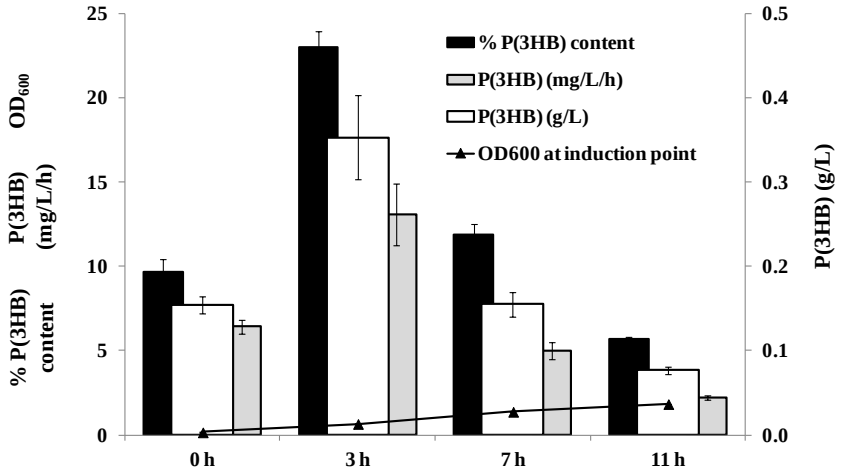

Figure 6.22 Effect of stage of cell at the induction point on P(3HB) biosynthesis.

E. coli-ABC$_{Ah}$ was cultivated in minimum medium containing glycerol as a sole carbon source. 1 mM IPTG was added into the culture medium at four different stages of cell [at initial inoculation (0 h), early log phase (3 h), mid log phase (7 h), and late log phase (11 h)]. After induction cells were cultivated for further 24 h. The amount of P(3HB) were analyzed by HPLC. Result is the average value and error bar represents standard deviation for triplicate experiments.

6.2.2 SCL-MCL-PHAs biosynthesis

Next, the ability of recombinant *E. coli* strains to synthesize SCL-MCL-PHAs was examined. By cross combinational co-expression of PhaAB with each of three PhaCs and three PhaJs, nine recombinant *E. coli* strains were generated: *E. coli*-ABC$_{Re}$J1$_{Pp}$, *E. coli*-ABC$_{Re}$J4$_{Pp}$, *E. coli*-ABC$_{Re}$J$_{Ah}$, *E. coli*-ABC$_{Ah}$J1$_{Pp}$, *E. coli*-ABC$_{Ah}$J4$_{Pp}$, *E. coli*-ABC$_{Ah}$J$_{Ah}$, *E. coli*-ABC2$_{Pp}$J1$_{Pp}$, *E. coli*-ABC2$_{Pp}$J4$_{Pp}$, and *E. coli*-ABC2$_{Pp}$J$_{Ah}$.

6.2.2.1 Effect of different PhaC and PhaJ types on SCL-MCL-PHAs biosynthesis

The ability of recombinant strains to convert glycerol to SCL-MCL-PHAs was evaluated by culturing in 300 mL M9 medium containing 2% (v/v) glycerol as a carbon substrate. IPTG (1mM) and sodium dodecanoate (1 g/L) were added to the culture media at 3 h after inoculation. The protein expression profiles were determined for *E. coli*-ABC$_{Re}$J1$_{Pp}$, *E. coli*-ABC$_{Ah}$J1$_{Pp}$, and *E. coli*-ABC2$_{Pp}$J1$_{Pp}$ (Fig 6.23), for *E. coli*-ABC$_{Re}$J4$_{Pp}$, *E. coli*-ABC$_{Ah}$J4$_{Pp}$, and *E. coli*-ABC2$_{Pp}$J4$_{Pp}$ (Fig 6.24), and for *E. coli*-ABC$_{Re}$J$_{Ah}$, *E. coli*-ABC$_{Ah}$J$_{Ah}$, and *E. coli*-ABC2$_{Pp}$J$_{Ah}$ (Fig 6.25). The contents and the compositions of produced copolymers were determined by HPLC. The method for preparation of samples for HPLC analysis was different between P(3HB) and SCL-MCL-PHA copolymer analysis. For analysis of accumulated P(3HB) content, dried cells were digested with H_2SO_4 (138) but this method cannot be used to analyze the compositions of SCL-MCL-PHA copolymer. For analysis of SCL-MCL-PHA copolymer compositions, dried cells were digested with NaOH (139). Figure 6.26 showed the comparison result of HPLC peaks. When P(3HB-6.9 mol% 3HHx) (Nodax) was digested with H_2SO_4, only C4 peak appeared. However, when P(3HB-6.9 mol% 3HHx) was digested with NaOH, both C4 and C6 peaks were detected.

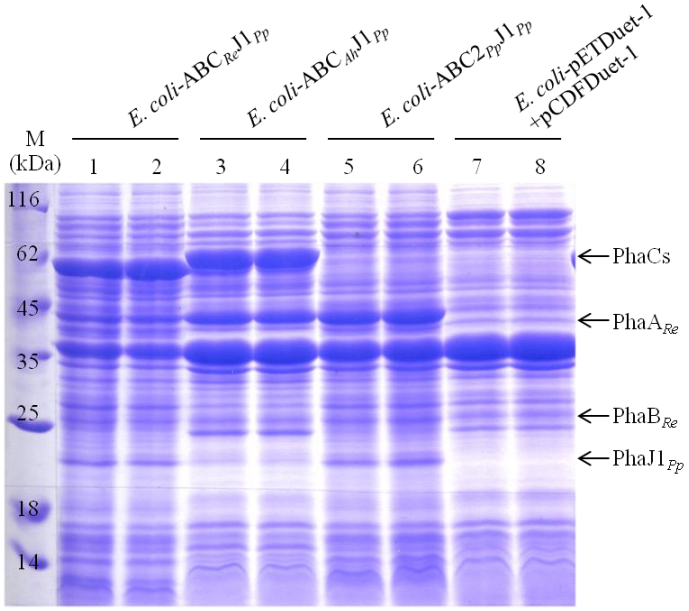

Figure 6.23 Protein expression profiles of *E. coli*-ABC$_{Re}$J1$_{Pp}$, *E. coli*-ABC$_{Ah}$J1$_{Pp}$, and *E. coli*-ABC2$_{Pp}$J1$_{Pp}$ as analyzed by SDS-PAGE.

SDS-PAGE analysis of protein profiles of *E. coli*-ABC$_{Re}$J1$_{Pp}$, *E. coli*-ABC$_{Ah}$J1$_{Pp}$, and *E. coli*-ABC2$_{Pp}$J1$_{Pp}$ cultured in M9 medium containing 2% (v/v) glycerol supplemented with yeast extract and sodium dodecanoate (1 g/L). The cells were induced with 1 mM IPTG after 3 h inoculation and harvested after 24 h. Lane M is Unstained Protein molecular weight marker. Lanes 1-2, 3-4, 5-6, and 7-8 are the proteins from *E. coli*-ABC$_{Re}$J1$_{Pp}$, *E. coli*-ABC$_{Ah}$J1$_{Pp}$, *E. coli*-ABC2$_{Pp}$J1$_{Pp}$, and *E. coli*-pETDuet-1+pCDFDuet-1, respectively. The expected size of PhaA$_{Re}$, PhaB$_{Re}$, PhaC$_{Re}$, PhaC$_{Ah}$, PhaC2$_{Pp}$, and PhaJ1$_{Pp}$ are 42 kDa, 27 kDa, 66 kDa, 68 kDa, 64 kDa, and 19 kDa, respectively. Arrows indicate the expressed recombinant proteins. The samples were loaded at equivalent OD_{600}.

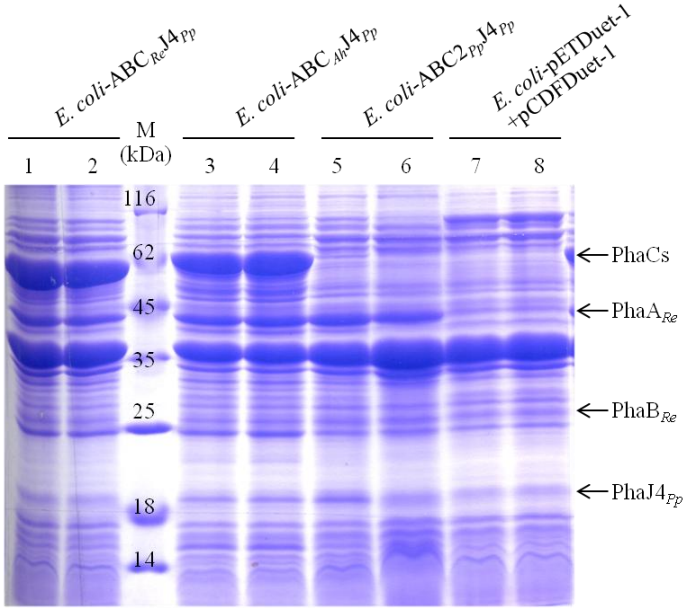

Figure 6.24 Protein expression profiles of *E. coli*-ABC$_{Re}$J4$_{Pp}$, *E. coli*-ABC$_{Ah}$J4$_{Pp}$, and *E. coli*-ABC2$_{Pp}$J4$_{Pp}$ as analyzed by SDS-PAGE.

SDS-PAGE analysis of protein profiles of *E. coli*-ABC$_{Re}$J4$_{Pp}$, *E. coli*-ABC$_{Ah}$J4$_{Pp}$, and *E. coli*-ABC2$_{Pp}$J4$_{Pp}$ cultured in M9 medium containing 2% (v/v) glycerol supplemented with yeast extract and sodium dodecanoate (1 g/L). The cells were induced with 1 mM IPTG after 3 h inoculation and harvested after 24 h. Lane M is Unstained Protein molecular weight marker. Lanes 1-2, 3-4, 5-6, and 7-8 are the proteins from *E. coli*-ABC$_{Re}$J4$_{Pp}$, *E. coli*-ABC$_{Ah}$J4$_{Pp}$, *E. coli*-ABC2$_{Pp}$J4$_{Pp}$, and *E. coli*-pETDuet-1+pCDFDuet-1, respectively. The expected size of PhaA$_{Re}$, PhaB$_{Re}$, PhaC$_{Re}$, PhaC$_{Ah}$, PhaC2$_{Pp}$, and PhaJ4$_{Pp}$ are 42 kDa, 27 kDa, 66 kDa, 68 kDa, 64 kDa, and 18 kDa, respectively. Arrows indicate the expressed recombinant proteins. The samples were loaded at equivalent OD_{600}.

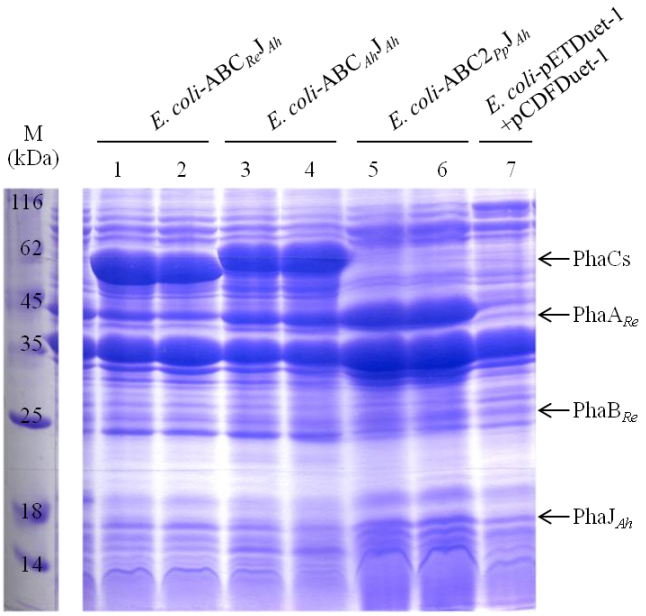

Figure 6.25 Protein expression profiles of *E. coli*-ABC$_{Re}$J$_{Ah}$, *E. coli*-ABC$_{Ah}$J$_{Ah}$, and *E. coli*-ABC2$_{Pp}$J$_{Ah}$ as analyzed by SDS-PAGE.

SDS-PAGE analysis of protein profiles of *E. coli*-ABC$_{Re}$J$_{Ah}$, *E. coli*-ABC$_{Ah}$J$_{Ah}$, and *E. coli*-ABC2$_{Pp}$J$_{Ah}$ cultured in M9 medium containing 2% (v/v) glycerol supplemented with yeast extract and sodium dodecanoate (1 g/L). The cells were induced with 1 mM IPTG after 3 h inoculation and harvested after 24 h. Lane M is Unstained Protein molecular weight marker. Lanes 1-2, 3-4, 5-6, and 7 are the proteins from *E. coli*-ABC$_{Re}$J$_{Ah}$, *E. coli*-ABC$_{Ah}$J$_{Ah}$, *E. coli*-ABC2$_{Pp}$J$_{Ah}$, and *E. coli*-pETDuet-1+pCDFDuet-1, respectively. The expected size of PhaA$_{Re}$, PhaB$_{Re}$, PhaC$_{Re}$, PhaC$_{Ah}$, PhaC2$_{Pp}$, and PhaJ$_{Ah}$ are 42 kDa, 27 kDa, 66 kDa, 68 kDa, 64 kDa, and 16 kDa, respectively. Arrows indicate the expressed recombinant proteins. The samples were loaded at equivalent OD_{600}.

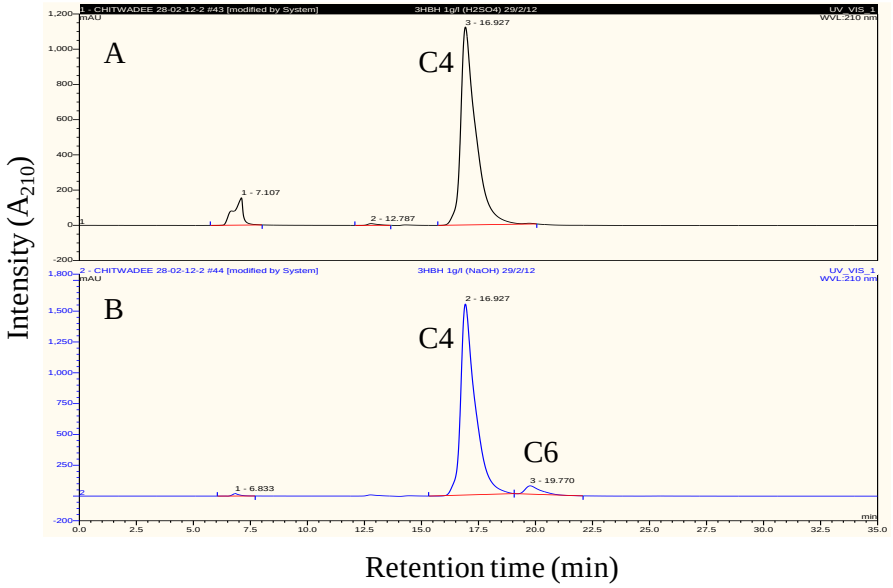

Figure 6.26 HPLC analysis of P(3HB-6.9 mol% 3HHx).

The polymers were digested with (A) H_2SO_4 or (B) 1N NaOH. C4 stands for 3HB-derived peak (crotonic acid). C6 stands for 3HHx-derived peak (hexenoic acid). The samples were analyzed by high performance liquid chromatography (HPLC) on an Ultimate 3000 standard LC system (Dionex, Sunnyvale, CA) equipped with a UV detector and an Aminex HPX-87H column (300 mm x 7.8 mm I.D) (Bio-Rad, Hercules, CA) operated at 55^{o}C at a flow rate of 0.5 mL/min. The mobile phase was 20% CH_3CN in 5 mM H_2SO_4 and chromatogram signals were detected at 210 nm.

HPLC analysis showed that *E. coli* expressing PhaABCs were able to produce SCL-MCL-PHA copolymers but the % mole fractions of the MCL-units were very low (less than 1 mol%). Whereas co-expression of PhaABCs and three different PhaJs resulted in the biosynthesis of various SCL-MCL-PHA copolymers consisting of monomers varying from C4 to C10 with various fraction of MCL-units up to 64 mol% (Table 6.3).

Next, some factors that may influence the molar fraction of MCL-unit and % content of produced copolymers were investigated since the molar fraction of MCL-unit in the polymer influences the properties of polymer. These included time-dependent change and concentration of dodecanoate. The candidate strain was *E. coli*-ABC$_{Ah}$J$_{Ah}$ which produced P(3HB-*co*-3HHx) copolymer at the highest content with highest 3HHx molar fraction.

Table 6.3 PHA copolymers biosynthesis from glycerol and dodecanoate in recombinant *E. coli* harboring *phaABC*s and *phaABCsJ*s [reproduced from (19) with permission from JSBA].

Strains	PHA content (wt% of CDW)	PHA monomer composition (mol%)			
		3HB	3HHx	3HO	3HD
E. coli-ABC$_{Ah}$	1.1 ± 0.37	99.4 ± 0.05	0.6 ± 0.05	-	-
E. coli-ABC$_{Re}$	0.5 ± 0.09	99.1 ± 0.1	0.85 ± 0.1	0.05 ± 0.02	-
E. coli-ABC2$_{Pp}$	trace	nd	nd	nd	nd
E. coli-ABC$_{Ah}$J1$_{Pp}$	1.0 ± 0.17	96 ± 0.4	4 ± 0.4	-	-
E. coli-ABC$_{Ah}$J4$_{Pp}$	1.7 ± 0.49	98 ± 0.3	2 ± 0.3	-	-
E. coli-ABC$_{Ah}$J$_{Ah}$	1.7 ± 0.66	96 ± 1.5	4 ± 1.5	-	-
E. coli-ABC$_{Re}$J1$_{Pp}$	3.2 ± 0.96	99.6 ± 0.1	0.4 ± 0.1	-	-
E. coli-ABC$_{Re}$J4$_{Pp}$	1.0 ± 0.21	96 ± 0.3	2 ± 0.4	2 ± 0.3	-
E. coli-ABC$_{Re}$J$_{Ah}$	0.8 ± 0.37	96 ± 0.6	3 ± 0.8	1 ± 0.4	-
E. coli-ABC2$_{Pp}$J1$_{Pp}$	0.1 ± 0.02	52 ± 4.9	7 ± 3.2	30 ± 1.5	11 ± 2.1
E. coli-ABC2$_{Pp}$J4$_{Pp}$	0.1 ± 0.01	65 ± 7.5	6 ± 1.9	16 ± 5.8	13 ± 3.3
E. coli-ABC2$_{Pp}$J$_{Ah}$	0.1 ± 0.01	36 ± 4.6	25 ± 1.6	30 ± 1.0	9 ± 3.9

Cells were cultivated at 37°C in M9 minimum medium containing 2% (v/v) glycerol as the sole carbon source supplemented with 1 g/L Bacto-yeast extract. After 3 h of cultivation, IPTG (1mM), sodium dodecanoate (1 g/L) and Brij-35 (2 g/L) were added and cells were grown for an additional 24 h. Results are the average ± standard deviations from four replications. 3HB, 3-hydroxybutyrate; 3HHx, 3-hydroxyhexanoate; 3HO, 3-hydroxyoctanoate; 3HD, 3-hydroxydecanoate; CDW, cell dry weight; -, not detectable; nd, not determined.

6.2.2.2 Effect of cultivation time on the P(3HB-*co*-3HHx) biosynthesis by *E. coli*-ABC$_{Ah}$J$_{Ah}$

PHA polymers are produced and accumulated inside the bacterial cells as insoluble granules; therefore the time-dependent change of PHA biosynthesis was investigated. *E. coli*-ABC$_{Ah}$J$_{Ah}$ was cultivated in 75 mL M9 minimum medium containing 2% (v/v) glycerol with yeast extract. Sodium dodecanoate (1 g/L) was added into the culture media together with 1mM IPTG after 3 h inoculation. The cells were collected at intervals to measure pH, OD_{600}, % PHA content and mol% 3HHx (Fig 6.27).The results showed that after 1 mM IPTG and dodecanoate (1 g/L) were added into the culture media, P(3HB-*co*-3HHx) was gradually accumulated and reached the maximum content at 3.5 wt% of CDW after cultivation for 34 h. The 3HHx fraction reached the maximum at 3 mol% after cultivation for 27 h and then decreased to 1.4 mol% after 34 h and was stable there up to 56 h. pH was decreased from 6.8 at 27 h to 6.1 at 34 h when cells entered into the stationary phase as indicated by OD_{600}.

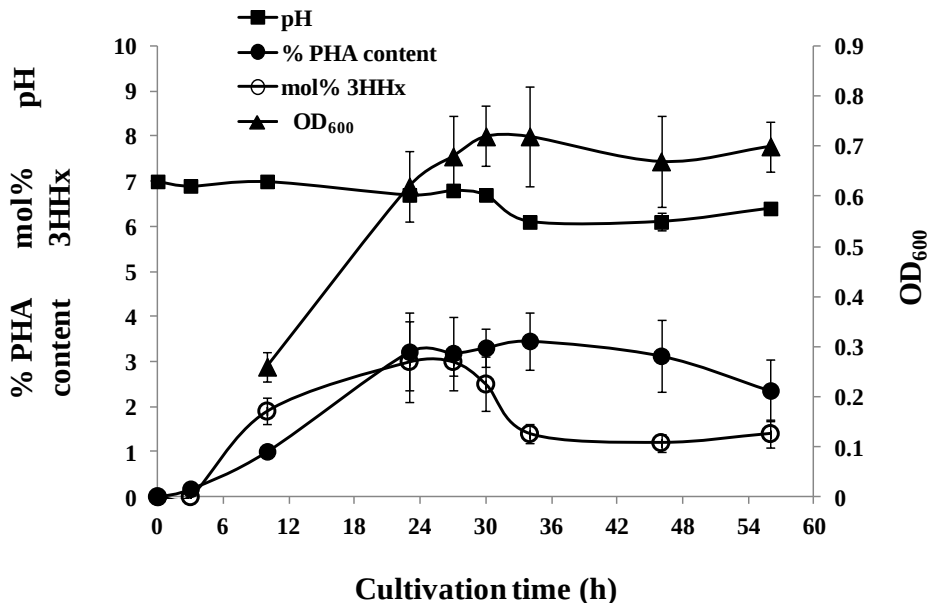

Figure 6.27 Time-dependent change in OD_{600}, pH, % PHA content, and mol% 3HHx.

E. coli-$ABC_{Ah}J_{Ah}$ was cultivated at 37°C in M9 minimum medium containing 2% (v/v) glycerol as the sole carbon source supplemented with Bacto-yeast extract (1 g/L). After 3 h of cultivation, IPTG (1mM), sodium dodecanoate (1 g/L) and Brij-35 (2 g/L) were added. Cells were harvested at interval time to measure OD_{600}, pH, % PHA content, and compositions. Results are the average ± standard deviations from three independent experiments.

6.2.2.3 Effect of dodecanoate concentration on the P(3HB-*co*-3HHx) biosynthesis by *E. coli*-ABC$_{Ah}$J$_{Ah}$

Based on our established hybrid biosynthesis pathway, fatty acid was supplied as the precursor of MCL-monomer. The intermediate of fatty acid β-oxidation was converted to MCL-monomer by the activity of PhaJ. Therefore the amount of dodecanoate (fatty acid) was varied to evaluate its effect on the mol% 3HHx (MCL-unit). *E. coli*-ABC$_{Ah}$J$_{Ah}$ was cultured in M9 minimum medium containing glycerol as a carbon source supplemented with yeast extract. After cultivation for 3 h, sodium dodecanoate was added into the culture media at 0.5, 1.0, and 1.5 g/L together with 1mM IPTG. They were cultured for additional 24 h then harvested. PHA content and its compositions were analyzed by HPLC (Table 6.4). The results revealed that cell dry weight, % PHA content, and its compositions were affected by the amount of sodium dodecanoate. When sodium dodecanoate concentration was increased, cell dry weight and % PHA content were decreased; whereas, the molar fraction of 3HHx was increased. The molar fraction of 3HHx was increased from 2 mol% to 5 mol% when sodium dodecanoate was increased from 0.5 g/L to 1.5 g/L.

Table 6.4 Effect of sodium dodecanoate concentration on PHA production.

Media	CDW (g/L)	PHA content (wt% of CDW)	PHA monomer composition (mol%)	
			3HB	3HHx
A	0.6 ± 0.18	4.6 ± 2.9	98 ± 0.8	2 ± 0.8
B	0.5 ± 0.11	3.4 ± 1.1	97 ± 0.5	3 ± 0.5
C	0.4 ± 0.23	1.5 ± 0.4	95 ± 1.2	5 ± 1.2

E. coli-ABC$_{Ah}$J$_{Ah}$ was cultivated at 37°C in M9 minimum medium containing 2% (v/v) glycerol as the sole carbon source supplemented with Bacto-yeast extract (1 g/L). After 3 h of cultivation, IPTG (1mM), sodium dodecanoate [(A) 0.5 g/L, (B) 1 g/L, (C) 1.5 g/L] and Brij-35 (2 g/L) were added and cells were grown for an additional 24 h. Results are the average ± standard deviations from four replications. 3HB, 3-hydroxybutyrate; 3HHx, 3-hydroxyhexanoate.

6.3 Using crude glycerol as a carbon source for PHAs biosynthesis

A surplus of glycerol generated as by-product from the growing biodiesel industry is a promising inexpensive carbon source (18). Since the high cost of PHAs is their major drawback which limits their used in daily-use plastic products. Thus it is interesting to determine if such crude glycerol can be used as a carbon source to reduce the production cost of PHAs. Two recombinant strains equipped with *phaABC* and *phaABCJ* were used in this experiment. The first strain was *E. coli*-ABC$_{Ah}$ which produced P(3HB) homopolymer from pure glycerol at the highest content than the other strains. The second strain was *E. coli*-ABC$_{Ah}$J$_{Ah}$ which produced P(3HB-*co*-3HHx) copolymer from pure glycerol at the highest content with highest 3HHx molar fraction.

6.3.1 Characterization of crude glycerol compositions

Crude glycerol in this study was obtained from a local biodiesel production plant which was the by-product of alkaline (NaOH)-catalyzed transesterification of palm oil with methanol (Trang Palm Oil Co. Ltd., Trang, Thailand). The crude glycerol was brown in color (Fig 6.28A). Its viscousity was similar to pure glycerol. After adding crude glycerol into M9 minimum medium, the medium turned to white (Fig 6.28B) which was different from clear M9 minimum medium with pure glycerol. Crude glycerol, as expected, composed of glycerol as a major component [81.1% (w/w)] with impurities of methanol [0.98% and 0.36% (v/v) of before and after autoclaving at 121^{o}C for 15 min, respectively], sodium [0.01% (w/w)], potassium [1.9% (w/w)] and trace amounts of monoglyceride [0.03% (w/w)], diglyceride [0.02% (w/w)], and triglyceride [0.07% (w/w)] (Table 6.5). The possibility of using this crude glycerol as a carbon source for culturing *E. coli*-ABC$_{Ah}$ and *E. coli*-ABC$_{Ah}$J$_{Ah}$ recombinant strains was investigated. *E. coli*-ABC$_{Ah}$ and *E. coli*-ABC$_{Ah}$J$_{Ah}$ were cultivated in shake flask using 1, 3, and 5% (v/v) crude glycerol as a sole carbon source to examine the effect of crude glycerol concentration on their growth (Fig 6.29). Both strains were able to grow using only crude glycerol as a carbon source. When concentration of crude glycerol was increased from 1 to 5% (v/v), there was no significant effect on cell dry weight (CDW) of *E. coli*-ABC$_{Ah}$

but there was a slight effect on CDW of *E. coli*-ABC$_{Ah}$J$_{Ah}$ after 24 h cultivation, with a slight decrease in CDW at higher glycerol concentration.

(A) **(B)**

Figure 6.28 The characteristic of crude glycerol produced from biodiesel production as a by-product.

(A) Crude glycerol from Trang Palm Oil Co. Ltd., Trang, Thailand. (B) M9 minimum medium containing 2% (v/v) crude glycerol.

Table 6.5 Compositions of crude glycerol.

Parameter	Crude glycerol	Unit
pH	8.9	
Glycerol	81.09	% (w/w)
Methanol (after auto clave)	0.36	% (v/v)
Monoglyceride	0.03	% (w/w)
Diglyceride	0.02	% (w/w)
Triglyceride	0.07	% (w/w)
Sodium	0.01	% (w/w)
Potassium	1.9	% (w/w)

(A)

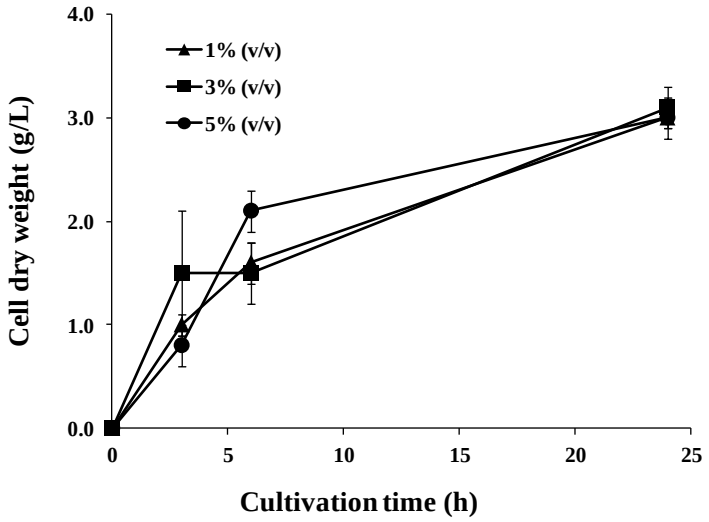

(B)

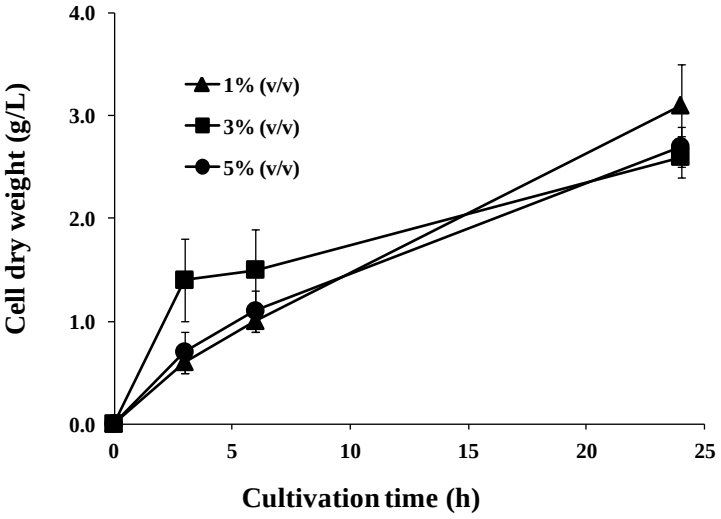

Figure 6.29 Growth profiles of recombinant *E. coli* cultured in crude glycerol [reproduced from (145) with permission from Springer].

(A) *E. coli*-ABC$_{Ah}$ and (B) *E. coli*-ABC$_{Ah}$J$_{Ah}$ were cultivated in shaking flask at 37^{o}C, 200 rpm using 1%, 3%, and 5% (v/v) crude glycerol as the carbon source. The cultured cells were collected at the interval time to measure the OD_{600}. Result is the average value and error bar represents standard deviation for triplicate experiment.

6.3.2 P(3HB) biosynthesis by *E. coli*-ABC$_{Ah}$

Next, the ability of *E. coli*-ABC$_{Ah}$ to use crude glycerol as a carbon source for biosynthesis of P(3HB) was investigated. *E. coli*-ABC$_{Ah}$ was cultivated in 75 mL M9 medium containing 1% (v/v) of crude glycerol or 1% (v/v) of pure glycerol as the carbon source. When crude glycerol was used, *E. coli*-ABC$_{Ah}$ produced P(3HB) content at 14 wt% of CDW which was less than when 1% of pure glycerol was used (26 wt% of CDW). However, the total CDW of *E. coli* cells cultured in crude glycerol was 4.0 g/L which was higher than that of pure glycerol (1.5 g/L). Therefore, the concentration of P(3HB) produced from crude glycerol (0.6 g/L) was higher than that of pure glycerol (0.4 g/L). In addition, the effect of crude glycerol concentration on the ability to synthesize P(3HB) by *E. coli*-ABC$_{Ah}$ was then investigated. Cells were cultured in 75 mL M9 medium containing 1% to 5% (v/v) of crude glycerol. The results showed that the maximum P(3HB) obtained was 13.9 wt% of CDW by using 1% (v/v) crude glycerol and gradually decreased to 1.6 wt% of CDW by using 5% (v/v) crude glycerol (Table 6.6). The decrease in P(3HB) content was in accordance with the expression level of recombinant proteins (Fig 6.30). When crude glycerol concentration was gradually increased, the expression level of PhaC and PhaA proteins was gradually decreased as evaluated by densitometer (Fig 6.31A and 6.31B, respectively).

Table 6.6 The effect of crude glycerol concentration on P(3HB) biosynthesis in *E. coli*-ABC$_{Ah}$ [modified from (145) with permission from Springer].

Crude glycerol (% v/v)	pH of media	CDW (g/L)	P(3HB) content (wt% of CDW)	P(3HB) (g/L)
1% (pure)	7.0	1.5 ± 0.25	25.5 ± 2.44	0.4 ± 0.07
1 %	7.1	4.0 ± 0.44	13.9 ± 2.52	0.6 ± 0.16
2 %	7.2	3.3 ± 0.17	9.6 ± 0.64	0.3 ± 0.07
3 %	7.3	3.2 ± 0.38	6.4 ± 0.66	0.2 ± 0.03
4 %	7.4	2.7 ± 0.32	3.8 ± 0.42	0.1 ± 0.01
5 %	7.5	2.8 ± 0.13	1.6 ± 0.10	0.05 ± 0.00

Cells were cultivated at 37°C in 75 mL M9 minimum medium containing glycerol as the sole carbon source supplemented with Bacto-yeast extract (1 g/L). After 3 h of cultivation, IPTG (1mM) was added and cells were grown for an additional 24 h. Results are the average ± standard deviations from four replications. CDW, cell dry weight.

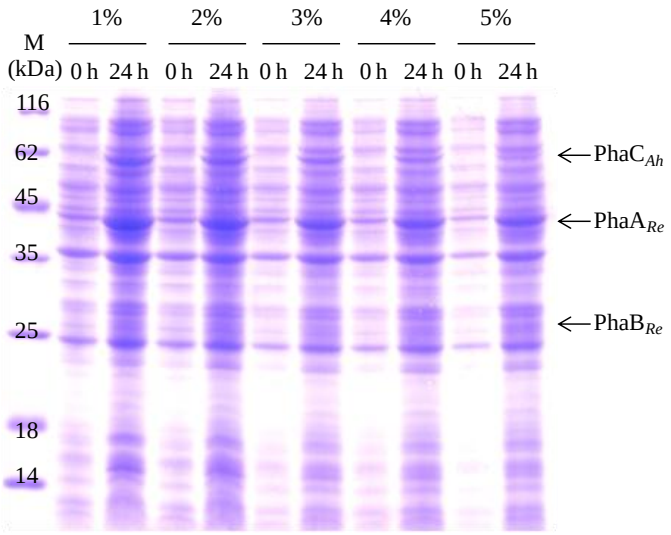

Figure 6.30 SDS-PAGE analysis of protein expression levels in *E. coli*-ABC$_{Ah}$ cultured in crude glycerol [reproduced from (145) with permission from Springer].

The recombinant cells were cultured in 75 mL M9 medium with different % of crude glycerol. The lanes indicated as 0 h represents expression profile at the induction time point (3 h after inculation). The lanes indicated as 24 h show the expression profile at 24 h after induction by 1 mM IPTG. The calculated sizes of PhaC$_{Ah}$, PhaA$_{Re}$, and PhaB$_{Re}$ are 68, 42, and 27 kDa, respectively and their expected migrations are indicated on the right. Arrows indicate the expected positions of recombinant proteins. The samples were loaded at equivalent cultured volume.

(A)

Crude glycerol	1%	2%	3%	4%	5%
PhaC intensity	1.00	0.80	0.75	0.72	0.4

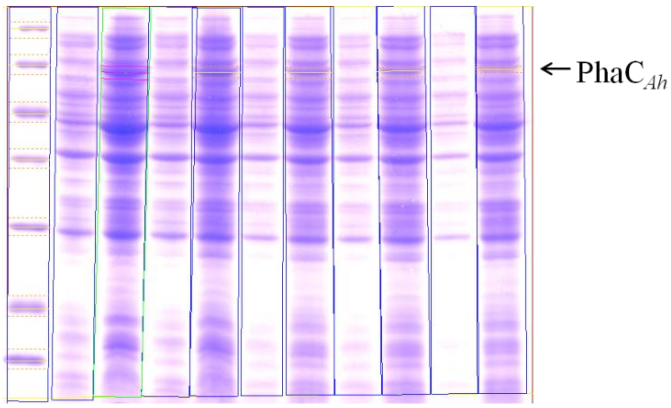

(B)

Crude glycerol	1%	2%	3%	4%	5%
PhaA intensity	1.00	0.86	0.81	0.72	0.65

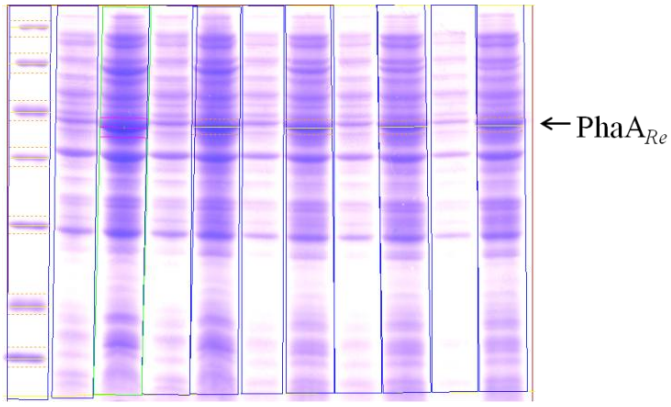

Figure 6.31 Densitometry analysis of protein band intensity.

Protein intensity level of PhaC$_{Ah}$ (A) and PhaA$_{Re}$ (B) expressed by *E. coli*-ABC$_{Ah}$ cultured in different crude glycerol concentration as a sole carbon source were analyzed by SynGene GeneTools (version: 4.03.02.0). The calculated relative intensity values of recombinant proteins are shown in the table.

6.3.3 P(3HB-*co*-3HHx) biosynthesis by *E. coli*-ABC$_{Ah}$J$_{Ah}$

To investigate the conversion of crude glycerol to P(3HB-*co*-3HHx), *E. coli*-ABC$_{Ah}$J$_{Ah}$ was cultured in 75 mL M9 medium containing 1% (v/v) crude glycerol as a sole carbon source. HPLC analysis revealed that by using crude glycerol as a sole carbon source, *E. coli*-ABC$_{Ah}$J$_{Ah}$ produced P(3HB) homopolymer (Table 6.7). Therefore, to provide precursors for MCL-monomer synthesis, fatty acid was added into the culture media. Here, sodium dodecanoate (1 g/L) was added at the induction time together with 1 mM IPTG and further incubated for 24 h. Cell dry weight, % PHA content, and PHA compositions were evaluated (Table 6.7). HPLC analysis showed that *E. coli*-ABC$_{Ah}$J$_{Ah}$ produced P(3HB-*co*-HHx) at 3 wt% of CDW with 1 mol% 3HHx fraction from crude glycerol which is less than 4 wt% of CDW with 3 mol% 3HHx fraction produced from pure glycerol. However, the total CDW of *E. coli* cells cultured in crude glycerol was 2.8 g/L which was higher than that of pure glycerol (0.9 g/L). Therefore, the concentration of produced P(3HB-*co*-3HHx) (g/L) from crude glycerol was higher than that of pure glycerol.

Table 6.7 PHA biosynthesis in *E. coli*-ABC$_{Ah}$J$_{Ah}$ using pure glycerol (PG) and crude glycerol (CG) with or without sodium dodecanoate (C12) [modified from (145) with permission from Springer].

Media	CDW (g/L)	PHA content (wt% of CDW)	PHA monomer composition (mol%)	
			3HB	3HHx
PG	1.6 ± 0.09	15.9 ± 0.31	100	-
CG	2.4 ± 0.13	6.6 ± 0.77	100	-
PG + C12	0.9 ± 0.16	4.3 ± 1.50	97 ± 1.5	3 ± 1.5
CG + C12	2.8 ± 0.59	2.9 ± 1.92	99 ± 0.3	1 ± 0.3

Cells were cultivated at 37°C in 75 mL M9 minimum medium containing 1 % (v/v) pure or crude glycerol as a carbon source supplemented with Bacto-yeast extract (1 g/L). After 3 h of cultivation, IPTG (1 mM) with or without sodium dodecanoate (1 g/L) were added and cells were grown for an additional 24 h. Results are the average ± standard deviations from three independent experiments. CDW, cell dry weight; -, not detectable.

6.4 PHA properties characterization

To investigate the effect of incorporated MCL-unit on their polymer properties, some PHAs produced [SCL-PHA: P(3HB) homopolymer produced from pure glycerol by *E. coli*-ABC$_{Re}$; and SCL-MCL-PHAs: P(3HB-1 mol% 3HHx) and P(3HB-3 mol% 3HHx) produced from crude and pure glycerol by *E. coli*-ABC$_{Ah}$J$_{Ah}$, respectively] were further characterized.

6.4.1 Chemical structure analysis by NMR

The extracted polymer polymers were dried under vacuum prior to characterize by ^{1}H NMR and ^{13}C NMR analysis. The NMR spectra of P(3HB-3 mol% 3HHx) copolymer was compared to that of P(3HB) homopolymer. P(3HB) exhibited three groups of chemical shifts (δ) in ^{1}H NMR at 1.23 ppm [3HB (3)], 2.45-2.60 ppm [3HB (1)], and 5.23 ppm [3HB (2)] for the methyl groups (-CH_3), the methylene groups (-CH_2), and the methine groups (-CH), respectively (Fig 6.32A). Whereas P(3HB-3 mol% 3HHx) exhibited the same spectral patterns as described above but with additional δ values of 0.83 ppm and 1.55 ppm, which represented the other positions of the terminal-CH_3 [3HHx (5)] and the internal-CH_2 [3HHx (3)], respectively, (Fig 6.32B). These results suggested that this polymer composed not only 3HB but also MCL-unit in the polymer chains. In addition, the ^{1}H NMR spectra intensity ratio of the main chain methylene proton resonance [3HB (1), 3HHx (1)] to methyl proton resonance [3HHx (5)] of copolymers were calculated to obtain the molar fractions of 3HB and 3HHx unit (Equation 1). The result corresponded to the HPLC analysis which indicated that 3 mol% 3HHx was incorporated into the polymer. Moreover, ^{13}C NMR spectra of P(3HB-3 mol% 3HHx) were consistent with the previously characterized P(3HB-*co*-3HHx) (146). The expanded spectra of carbonyl resonance between 169.2-169.7 ppm split to four peaks resulted from the different sequential connection of 3HB and 3HHx units (Fig 6.33B), in contrast to the only one peak of P(3HB) (Fig 6.33A).

Equation 1

$$\% \text{ molar fraction of 3HHx} = \left[\frac{\text{intensity of 3HHx (5) peak / 3}}{\text{(intensity of 3HB (1) + 3HHx (1)) / 2}} \right] \times 100$$

$$= \left[\frac{0.09 / 3}{(1.01 + 1.03) / 2} \right] \times 100 = 2.94\%$$

(A)

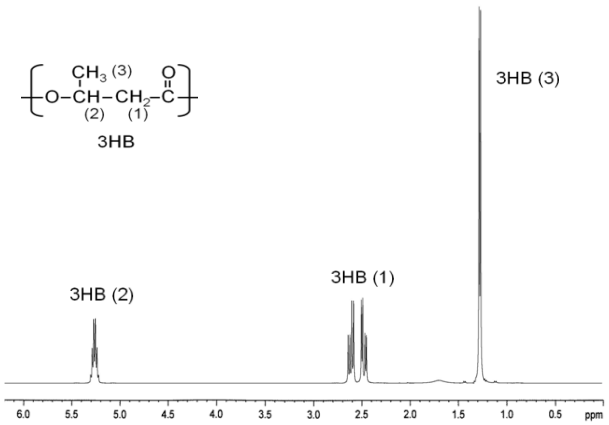

(B)

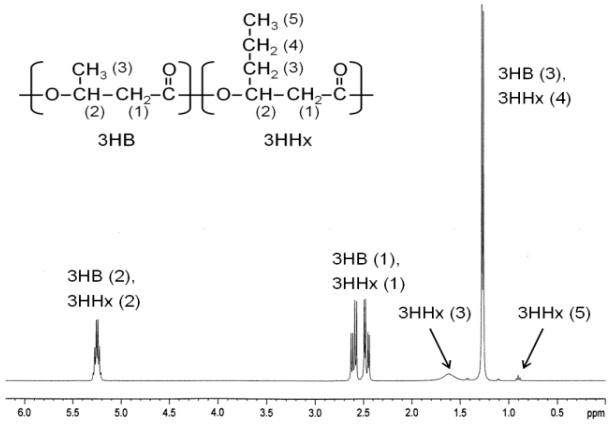

Figure 6.32 Chemical structure analysis of P(3HB) and P(3HB-3 mol% 3HHx) by ^{1}H NMR [reproduced from (145) with permission from Springer].

^{1}H NMR spectra of P(3HB) extracted from *E. coli*-ABC$_{Re}$ (A) compared to P(3HB-3 mol% 3HHx) copolymers extracted from *E. coli*-ABC$_{Ah}$J$_{Ah}$ (B).

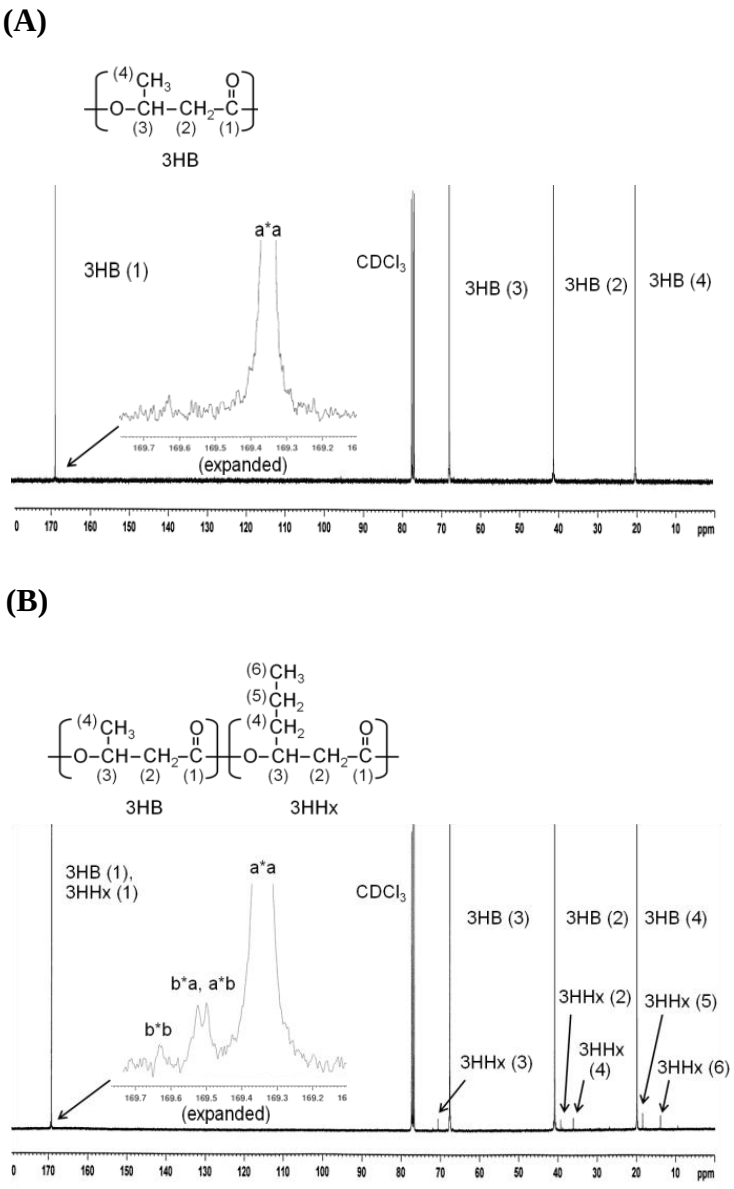

Figure 6.33 Chemical structure analysis of P(3HB) and P(3HB-3 mol% 3HHx) by ^{13}C NMR [reproduced from (145) with permission from Springer].

^{13}C NMR spectra of P(3HB) extracted from *E. coli*-ABC$_{Re}$ (A) compared to P(3HB-3 mol% 3HHx) copolymers extracted from *E. coli*-ABC$_{Ah}$J$_{Ah}$ (B). a*a, refers to 3HB connected to 3HB; a*b and b*a, refer to 3HB connected to 3HHx and vice versa; b*b, refers to 3HHx connected to 3HHx.

6.4.2 Molecular weight analysis by GPC

The molecular weight and the polydispersity index of PHAs produced were determined by GPC (Table 6.8). The average molecular weights (M_w) of P(3HB), P(3HB-1 mol% 3HHx), and P(3HB-3 mol% 3HHx) were in range of (1.1-2.6) x10^5 Da. Their polydispersity index which indicates their heterogeneousity with higher value, denoting greater heterogeneousity were around 2.0.

6.4.3 Thermal properties analysis by DSC

The thermal properties including glass transition temperature (T_g) and melting temperature (T_m) of P(3HB), P(3HB-1 mol% 3HHx), and P(3HB-3 mol% 3HHx) were determined by DSC (Table 6.8). T_g is the temperature at which the polymer is converted between glassy and rubbery states while T_m is the temperature at which the polymer is converted between rubbery and melting states. T_g values of P(3HB), P(3HB-1 mol% 3HHx), and P(3HB-3 mol% 3HHx) were 7.5^{o}C, 6.9^{o}C, and 5.5^{o}C, respectively. DSC thermogram of P(3HB) showed only one T_m peak at 175.0^{o}C (Fig 6.34A), while DSC thermogram of P(3HB-1 mol% 3HHx) showed one distinct T_m peak with a shoulder at 174.3^{o}C (Fig 6.34B). On the other hand, DSC thermograms of P(3HB-3 mol% 3HHx) showed two T_m peaks at 158.7^{o}C and 171.3^{o}C. These observed two peaks might be resulted from the heterogeneity of produced copolymer, the multiple crystalline forms, or due to the recrystallization during the heating runs in the DSC where the lower T_m peak is the real melting point of original crystals and the higher T_m peak is the melting point of crystal formed by recrystallization (147).

6.4.4 Degradation temperature analysis by TGA

P(3HB), P(3HB-1 mol% 3HHx) and P(3HB-3 mol% 3HHx) were characterized by thermogravimetry analysis (TGA) to evaluate their thermal degradation temperature (T_d). T_d is the temperature at which the polymer is started to loss of its physical, mechanical or electrical properties. The results showed that T_d value of P(3HB) homopolymer was 291.7^{o}C which was slightly lower than those of P(3HB-1 mol% 3HHx) and P(3HB-3 mol% 3HHx) copolymers (299.4^{o}C and 294.6^{o}C, respectively) (Table 6.8).

Table 6.8 Molecular weight and thermal properties of PHAs [modified from (145) with permission from Springer].

Type of PHAs	Molecular weight		Thermal properties (^{o}C)		
	M_w (x10^5)	PDI	T_g	T_m	T_d
P(3HB)	2.6	1.9	7.5	175.0	291.7
P(3HB-1 mol% 3HHx)	1.1	2.1	6.9	174.3	299.4
P(3HB-3 mol% 3HHx)	1.3	2.0	5.5	158.7, 171.3	294.6

M_w, weight average molecular weight; PDI, polydispersity index; T_g, glass transition temperature; T_m, melting temperature; T_d, degradation temperature.

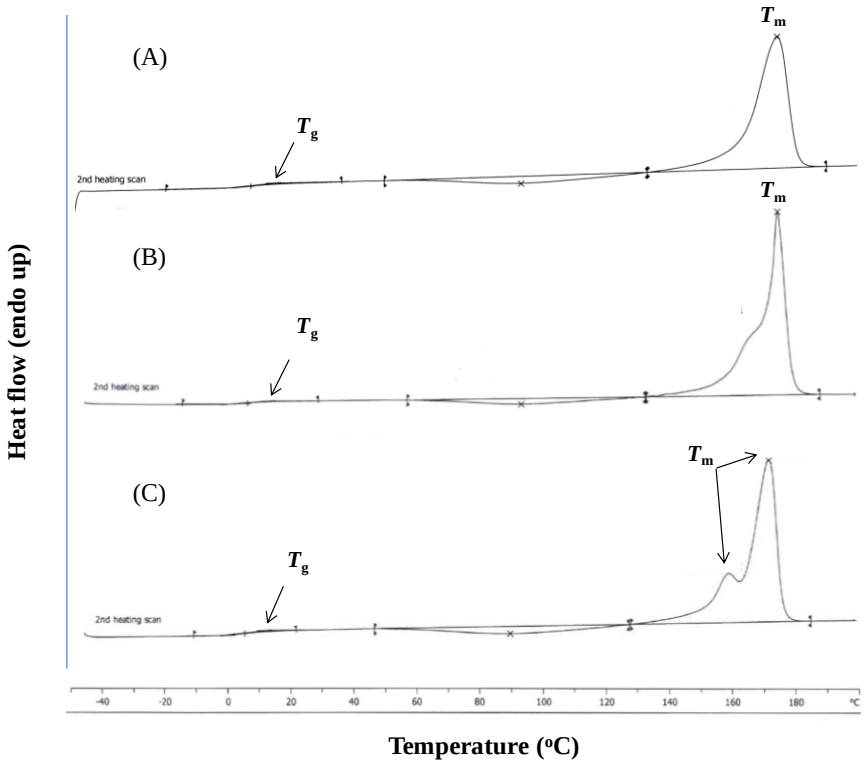

Figure 6.34 DSC thermogram of PHAs.

P(3HB) (A), P(3HB-*co*-3HHx) extracted from *E. coli*-ABC$_{Ah}$J$_{Ah}$ cultured in pure (B) and crude glycerol (C). T_g, glass transition temperature; T_m, melting temperature**.**

CHAPTER VII
DISCUSSION

7.1 Establishment of PHA biosynthesis pathway in recombinant *E. coli*

The compositions of PHAs produced are dependent on three major factors which are the feeding substrate, the metabolic route for providing monomers and the activity of PHA synthase (38, 39). Since the compositions of PHAs influence the properties of polymer materials, the challenge is to produce controllable compositions of PHAs. In this thesis, the hybrid pathway which combines two monomer supplying routes mimicking from two groups of native PHA-producing bacteria and one polymerase enzyme which can polymerize both SCL-monomer and MCL-monomer was designed (Fig 1.2). The advantage of the hybrid pathway is that the fraction between SCL-unit and MCL-unit in SCL-MCL-PHA copolymer can be easily controlled by adjusting the concentration ratio of glycerol and fatty acid. This similar strategy was also used to control the fraction of 3HP and 4HB in P(3HP-*co*-4HB) produced from *E. coli* by using 1,3-propanediol and 1,4-butanediol as co-substrates (148). Other strategies can also control the ratio between SCL and MCL but are more complicated. For example, the fractions of 3HP and 3HB are controlled under different inducible promoters of their monomer supplying routes in recombinant *E. coli* for biosynthesis of P(3HP-*co*-3HB) from glycerol (149). The lactic acid fraction (LA) in P(LA-*co*-3HB) was regulated by site-specific mutagenesis of the polymerase enzyme (150). Moreover, in our study three different polymerase enzymes (PhaCs) and three different MCL-monomer supplying related enzymes (PhaJs) were varied. Therefore, a variation of compositions of produced PHA would be expected.

Two sets of recombinant plasmids were constructed which were pETDuet-*ABC*s and pCDFDuet-*J*s. First, *phaABC*s were cloned into the same vector since these three genes encode the enzymes for P(3HB) biosynthesis pathway. Next, *phaJ*s were cloned into pCDFDuet-1 vector and co-expressed with PhaABCs to

complete the pathway for biosynthesis of SCL-MCL-PHA copolymers. Recombinant *E. coli* strains could express all recombinant proteins (PhaABCsJs) as indicated by SDS-PAGE and western blot analysis. The expression level of three different PhaCs was different. It was found that PhaC2$_{Pp}$ was expressed at the lowest level. However, in cell expressing PhaC2$_{Pp}$, the expression level of PhaA was higher than that of the other two strains, probably because they share the common resource pool for protein biosynthesis.

7.2 Using pure glycerol as a carbon source for PHAs biosynthesis

In this study, *E. coli* was selected as a host strain for PHAs production due to several advantages such as the ability to utilize several carbon substrates, fast growth to high cell density, and lack of intracellular PHA depolymerase (78, 79). Native *E. coli* is unable to produce and accumulate PHA granules. Therefore, some strategies of metabolic engineering approaches which were heterologous gene expression and substrate precursor addition were applied to establish the bio-system for PHA biosynthesis in *E. coli* (81). PHA synthase (PhaC) which is the key enzyme for polymerization of the (*R*)-3-hydroxyacyl-CoA monomers to PHAs were varied. Different PhaC enzymes from three sources showed effect on the ability to produce P(3HB). Nile blue A fluorescence staining analysis suggested that *E. coli*-ABC$_{Re}$ and *E. coli*-ABC$_{Ah}$ accumulated PHA granules inside the cells (Fig 6.16). However, HPLC results revealed that all three strains: *E. coli*-ABC$_{Re}$, *E. coli*-ABC$_{Ah}$, and *E. coli*-ABC2$_{Pp}$ could produce and accumulate P(3HB) (Table 6.1). These differences between Nile blue A staining and HPLC analysis results may be due to the sensitivity limitation of Nile blue A staining. Under the cultured condition used, *E. coli*-ABC$_{Ah}$ accumulated P(3HB) as similar to *E. coli*-ABC$_{Re}$ at 30 wt% and 24 wt%, respectively. On the other hand, *E. coli*-ABC2$_{Pp}$ accumulated P(3HB) only at 2 wt% of CDW. Since PhaC2$_{Pp}$ was originated from *P. putida* KT2440 which was reported as a MCL-PHA producer (151), PhaC2$_{Pp}$ tends to prefer MCL-3HA-CoA monomers than (*R*)-3HB-CoA as substrate. This preference may cause low content of P(3HB) produced from *E. coli*-ABC2$_{Pp}$. Another possibility may be due to the low expression level of PhaC2$_{Pp}$ (Fig 6.15) as there is a report that the expression level of PhaC

correlates to the amount of P(3HB) produced (152). However, based on our results, the PhaC expression level and the amount of accumulated P(3HB) were correlated only when the same PhaC was used. Since $PhaC_{Ah}$ was expressed at lower level than $PhaC_{Re}$ but *E. coli*-ABC_{Ah} produced more P(3HB) than *E. coli*-ABC_{Re} (Fig 6.15). The results suggested that besides the expression level, the types of PhaCs which would have different specific activity may affect P(3HB) production.

Since *E. coli*-ABC_{Ah} gave highest P(3HB) content from glycerol, it was further used as a producer to investigate other cultivation parameters. The results suggested that the ability to synthesize P(3HB) by *E. coli*-ABC_{Ah} was not significantly affected by increasing the concentration of pure glycerol. This is because CDW, % P(3HB) content, and P(3HB) concentration were only slightly decreased at 1.2, 1.2, and 1.4 fold, respectively, with increasing glycerol concentration. The amount of glycerol remaining after 27 h cultivation indicated that the amount of glycerol used was in excess. On the other hand, when a common-use carbon source like glucose was used, less amount of P(3HB) was obtained than that obtained from glycerol used at the same concentration (g/L) and in excess amount. This might result from different carbon catabolism of glycerol and glucose. Since glycerol has lower oxidation state than glucose, its catabolism generates more reducing equivalents (NADH) and leads to the higher ratio of NADH/NAD+ (153). In order to maintain the redox balance, the cells have to drive carbon flow toward the synthesis of reduced products including P(3HB). Moreover, it is known that NADH significantly inhibits citrate synthase activity, thus causing more available acetyl-CoA molecules for P(3HB) biosynthesis (154). On the other hand, the pH of culture media after 27 h cultivation with glucose was lower than that of glycerol suggesting that, apart from P(3HB), other acids might be produced in the culture media with glucose. The addition of yeast extract into the culture media supported better growth of the cells but the amount of P(3HB) produced is decreased. This is not surprising as it is known that most of native PHA-producing strains accumulate PHA when growing in the nitrogen-limited media. These results suggested that P(3HB) biosynthesis in recombinant strain might be accelerated by high carbon/nitrogen ratio. Furthermore, it was suspected that the stage of cells at the induction time would influence the production of P(3HB). In fact, most of the investigations induce protein expression at early log phase (87, 155, 156) but some of

them induce at the initial (14, 157) or using a two-stage fed-batch culture dividing a cell growth phase and a P(3HB) accumulation phase (158). As expected, the P(3HB) productivity was highest when induced at early log phase of cells and less P(3HB) was found if induced at late log phase.

Also, the MCL monomers-supplying route was established by co-transformation of pCDFDuet-*J*s together with pETDuet-*ABC*s into *E. coli*. The biosynthesis of SCL-MCL-PHA copolymers from glycerol was investigated. *E. coli*-ABC$_{Ah}$, *E. coli*-ABC$_{Re}$, and *E. coli*-ABC2$_{Pp}$ were used as control strains. HPLC analysis revealed that co-expression of only PhaABC (without PhaJ) also produced SCL-MCL-PHA copolymers when dodecanoate was supplemented into the culture media (Table 6.3). This suggested that *E. coli* BL21(DE3) possesses some endogenous enzymes or some metabolic routes that can provide MCL-monomers for PHA synthase. Previous reports revealed that some enzymes of *E. coli* can catalyze the intermediates of fatty acid β-oxidation to MCL-3HA-CoA monomer molecules. For example, 3-ketoacyl-ACP reductase (FabG) from *E. coli* catalyzes 3-ketoacyl-CoA to (*R*)-3-HA-CoA (91) and MaoC form *E. coli* has PhaJ-like function by catalyzing 2-enoyl-CoA to (*R*)-3-HA-CoA (94). However, based on our result, only a small fraction of MCL-units (less than 1 mol%) were incorporated in the polymers, suggesting that the activity level of its endogenous enzyme was very low since this heterologous pathway has to compete with the inherent pathways for intermediates. Therefore, PhaJ enzymes were co-expressed with PhaABCs in recombinant *E. coli* to increase the fraction of MCL-units.

HPLC analysis indicated that co-expressing PhaA and PhaB with various PhaCs and PhaJs in recombinant *E. coli* (*E. coli*-ABCsJs) caused the strains to produce various SCL-MCL-PHA copolymers (Table 6.3). However, the % content values of PHA copolymers were not high (0.1-3.2 wt% of cell dry weight). By comparing the amount of PHA produced by *E. coli*-ABC$_{Ah}$ in the medium with or without dodecanoate, it was found that P(3HB) was accumulated at 22 wt% of CDW when 2% glycerol was used as a sole carbon source (Table 6.2), whereas when sodium dodecanoate was supplemented into the culture media % PHA content was dramatically decreased to only 1 wt% of CDW. This reduction might be due to the toxicity effect of fatty acid (dodecanoate) on the cell. The action of fatty acids on

bacterial cell still unclear, but the prime target seems to be the membrane and on various processes occurring at the membrane of bacteria (159, 160). Therefore one possible way to optimize the productivity is by using fed-batch cultivation approach to gradually feeding fatty acid into the culture media.

Considering the compositions of PHA produced, PhaC may be the most important factor in determining copolymer compositions. PHAs composing of 3HB (C4) and 3HHx (C6) were obtained from cell expressing PhaC$_{Ah}$ suggesting that PhaC$_{Ah}$ prefers to C4 and C6 monomers. This was not unexpected as it was reported that PhaC$_{Ac}$ prefers to C4 and C6 monomers (13, 95). Besides 3HB (C4) and 3HHx (C6), the longer monomer 3HO (C8) was detected in cells expressing PhaC$_{Re}$, this suggested that PhaC$_{Re}$ has broader substrate specificity than PhaC$_{Ah}$. Although native *R. eutropha* is reported to produce P(3HB) (140) and the *in vitro* study indicated that substrate specificity of PhaC$_{Re}$ is toward only SCL-monomers (161), our study revealed that in recombinant host equipped with the pathway providing both SCL-monomer and MCL-monomer, not only SCL-monomer but also MCL-monomer could be polymerized by PhaC$_{Re}$. While in cells expressing PhaC$_{Ah}$ or PhaC$_{Re}$ produced copolymers composing mainly 3HB-unit with a small fraction of MCL-unit (up to 4 mol%), cells expressing PhaC2$_{Pp}$ produced copolymers composing at least half of MCL-unit fraction (48-64 mol%) and longer monomer 3HD (C10) was also detected. This is the first study demonstrating the *in vivo* substrate specificity of PhaC2$_{Pp}$. The result suggested that PhaC2$_{Pp}$ could polymerize both SCL-monomer and MCL-monomers and has broader substrate specificity than PhaC$_{Ah}$ and PhaC$_{Re}$.

On the other hand, considering the effect of PhaJ on the compositions of PHAs produced, the result indicated that PhaJs provided various monomers up to ten carbon chain length (C10). Also, this study revealed, for the first time, the *in vivo* substrate specificity of PhaJ$_{Ah}$. Although native *A. hydrophila* ATCC 7966 produces PHA composed of 3HB (C4) and 3HHx (C6) (31), the substrate specificity of PhaJ$_{Ah}$ was not limited to only C4 and C6 but also the longer monomers. In addition, the PHA compositions in cells expressing PhaC2$_{Pp}$ (*E. coli*-ABC2$_{Pp}$J1$_{Pp}$, *E. coli*-ABC2$_{Pp}$J4$_{Pp}$, and *E. coli*-ABC2$_{Pp}$J$_{Ah}$) showed that the dominant monomers 3HO (C8) and 3HD (C10) were detected when cells expressed PhaJ1$_{Pp}$ and PhaJ4$_{Pp}$, whereas the shorter monomer 3HHx (C6) and 3HO (C8) were detected in cells expressing PhaJ$_{Ah}$. These

suggested that various PhaJ variants influenced the dominant MCL-monomer in the PHA produced. Therefore, the variable compositions of SCL-MCL-PHAs could be produced by matching different monomer supplying enzymes (PhaJs) with different polymerase enzymes (PhaCs).

Based on these results, one candidate strain, *E. coli*-ABC$_{Ah}$J$_{Ah}$ was selected to investigate its biosynthesis of P(3HB-*co*-3HHx) over time (56 h). The results indicated that the content and compositions of P(3HB-*co*-3HHx) in *E. coli*-ABC$_{Ah}$J$_{Ah}$ is time-dependent. After induction, the polymer content was gradually increased and reached the maximum when cell enter into the stationary phase. The fraction of 3HHx was sharply increased to the maximum at 3 mol% in the exponential growth phase. However, later, the 3HHx fraction was decreased to 1.4 mol%. This might be due to the less active β-oxidation in cell decreasing growth rate, the loss of recombinant plasmid, or the lesser amount of remaining dodecanoate after longer cultivation. It was then confirmed that the fraction of 3HHx was correlated to the amount of dodecanoate (Table 6.4). These suggested that, the fraction of MCL-units could be regulated by the amounts of fatty acid precursor substrate.

Taken together, these data demonstrated that the constructed recombinant *E. coli* strains are able to produce P(3HB) and SCL-MCL-PHAs by using pure glycerol as a carbon source.

7.3 Using crude glycerol as a carbon source for PHA biosynthesis

The compositions of crude glycerol depend on the starting materials, the method of transesterification, and the recovery process (109). Since crude glycerol used in this study was partially purified; it was quite pure, consisting of 81% glycerol with smaller fractions of impurities (methanol, salts, and mono-, di-, and triglycerides); this is in contrast to some other previously characterized crude glycerol sources which contained 63-77% glycerol and 23-38% methanol (162). The possibility of utilizing this crude glycerol as a carbon source for biosynthesis of PHAs by our constructed recombinant *E. coli* strains was investigated. The result indicated that *E. coli*-ABC$_{Ah}$ was able to grow using only crude glycerol as a carbon source. Moreover, the total cell dry weight of *E. coli* cells cultured in 1% (v/v) crude glycerol

was higher than that in pure glycerol. This suggested that some impurities in crude glycerol such as mono-, di-, triglyceride might enhance the bacterial growth. Teeka et al., (2010) also found that an unidentified bacteria strain, AIK7, grows better in crude glycerol (163). However, some previous studies found that some impurities especially sodium salt in crude glycerol suppressed the growth of bacteria (2, 130). Since our crude glycerol contained small amount of sodium salt ~0.01% (w/w), this might not affect cell growth. However, when the concentration of crude glycerol was gradually increased from 1% to 5% (v/v), the concentration of P(3HB) was gradually decreased from 14 wt% to 2 wt% of CDW, respectively. Furthermore, the expression level of recombinant proteins was also decreased with increasing crude glycerol concentration. These suggested that in the recombinant strains, crude glycerol concentration affected the expression level of recombinant proteins which then directly influence the amount of accumulated P(3HB). On the other hand, the decrease in protein expression level and P(3HB) productivity could have resulted from the effect of higher osmotic stress on the cells and/or the effect of some conditions such as higher pH and salts that might impede recombinant proteins expression and polymer biosynthesis (164). It should be noted that when the concentration of pure glycerol was increased from 1% to 5% (v/v), the % P(3HB) content was only slightly decreased (1.2 fold); whereas, when the concentration of crude glycerol was increased from 1% to 5% (v/v), the % P(3HB) content was significantly decreased (8.7 fold).

Based on this result, 1% (v/v) crude glycerol was then tested for its possibility to use as a carbon source for biosynthesis of P(3HB-*co*-3HHx) copolymer by *E. coli*-ABC$_{Ah}$J$_{Ah}$. When crude glycerol was used, *E. coli*-ABC$_{Ah}$J$_{Ah}$ only produced P(3HB) homopolymer, indicating that using just crude glycerol cannot lead to the production of SCL-MCL-PHAs. This is in contrast to the previous study which demonstrated that *Pseudomonas corrugata* can use crude glycerol as a sole carbon source for biosynthesis of MCL-PHA suggesting that fatty acid precursors remaining in crude glycerol undergoes β-oxidation to provide MCL-monomers (132). It should be noted that crude glycerol used in that contains fatty acid soap, fatty acid methyl ester, mono-, and di-glyceride in total at 34% which were approximately 300 times higher than that present in the crude glycerol used in our study (mono-, di-, tri-glycerides in total at 0.12%). Therefore, it is possible that the fatty acid precursors

remaining in our crude glycerol might not be enough to be converted to MCL-monomers for copolymer biosynthesis. By adding dodecanoate into the culture media, recombinant *E. coli*-ABC$_{Ah}$J$_{Ah}$ is able to produce P(3HB-*co*-HHx) copolymer as expected. The results suggest that crude glycerol used in this study has a potential to use as a carbon source for recombinant cells growth and PHAs biosynthesis.

7.4 PHA properties characterization

The weight average molecular weight (M_w) values of P(3HB), P(3HB-1 mol% 3HHx), and P(3HB-3 mol% 3HHx) produced in this study were in the degree of 10^5 Da suggesting that the recombinant strains produced high molecular weight polymers comparable to the previous studies using glycerol for PHA biosynthesis (122, 131, 165). However these obtained values were slightly lower than those obtained from copolymers produced by recombinant *E. coli* using glucose as a carbon source [(4.6-6.5) x 10^5 Da] (166). According to the previous studies, it has been demonstrated that lower M_w of PHAs (122, 124, 131) was because glycerol can act as an end-cap to terminate the polymerization reaction (167).

On the other hand, incorporation of 3HHx fraction into the polymer causes changes in the thermal properties of produced PHAs. The results showed that glass transition temperature (T_g) values were inversely correlated to the 3HHx fraction (Table 6.8), in which increasing 3HHx fraction decreased the values of T_g. In general, the lower T_g values are resulted from the higher of the segmental mobility of polymer chains (147, 168). Therefore, the incorporation of 3HHx unit, which contains longer flexible side-chain than 3HB, resulted in copolymers with higher segmental mobility. In addition, the incorporation of 3HHx unit also affected the melting temperature (T_m) of polymers in which increasing 3HHx fraction resulted in decreasing T_m of P(3HB-*co*-3HHx) copolymers. This result suggested that the crystallinity of P(3HB) homopolymer was decreased by 3HHx incorporation. Since typical PHAs suffer from thermal degradation during the melting process (168), increasing the gap between melting temperature and thermal decomposition temperature is required. Therefore the lower T_m of P(3HB-*co*-3HHx) copolymer is advantageous because the material

melting process can be carried out at lower temperature than its thermal decomposition condition.

Moreover, the results of TGA analysis showed that a small fraction of 3HHx incorporated in the polymers slightly increased their thermal degradation temperature (T_d), up to 299^{o}C. During thermal degradation, P(3HB) undergoes a random chain scission via β-hydrogen transfer through the formation of a six-membered ring intermediate (169). Therefore, the steric hindrance of propyl side chain of 3HHx might disturb the formation of six-membered ring which causes the increase in the thermal degradation temperature of P(3HB-*co*-3HHx) when compared to P(3HB). However, the difference was not significant as the fraction of 3HHx was not high. Besides the MCL-unit fraction that affects the thermal stability of polymers, the presence of some impurities, such as some fermentation residues or some salts in polymers, may also affect the thermal stability (169, 170). Considering the T_d values of P(3HB), P(3HB-1 mol% 3HHx), and P(3HB-3 mol% 3HHx) extracted from the recombinant strains in this study, the results indicated that T_d of these PHAs are superior than those of previously obtained from P(3HB) produced from glycerol by *Burkholderia cepacia* (281.5^{o}C) (124) or from P(3HB-*co*-3HHx) produced from wheat germ oil by *A. hydrophila* 7966 (~250^{o}C) (31). Taken together, the results suggested that the PHA polymers produced from either pure or crude glycerol by our recombinant *E. coli* possess the properties suitable for various industrial applications such as softeners, pharmaceutical agents, and also in some nano-particles (130, 171, 172).

CHAPTER VIII
CONCLUSIONS

In this study, the recombinants *E. coli* with ability to convert glycerol to PHAs have been successfully developed. The recombinant *E. coli* strains harboring β-ketothiolase (PhaA) and acetoacetyl-CoA reductase (PhaB) from *R. eutropha* and a PHA synthase enzyme (PhaC) from either *R. eutropha*, *A. hydrophila*, or *P. putida* showed the ability to utilize glycerol as a sole carbon source for biosynthesis of P(3HB). The difference in the expression level and the specific activity/substrate specificity of the three PhaCs influence the amount of accumulated P(3HB). Under the same cultivation conditions, cells expressing PhaAB with PhaC from *R. eutropha* (*E. coli*-ABC$_{Re}$) or PhaC from *A. hydrophila* (*E. coli*-ABC$_{Ah}$) produced similar amount of P(3HB); whereas, cells expressing PhaAB with PhaC2 from *P. puida* (*E. coli*-ABC2$_{Pp}$) produced the lowest amount of P(3HB). The cultivation parameters including types of carbon source, carbon: nitrogen ratio, and the stage of the cells at the induction point are found to be important for further optimization of P(3HB) production. Using glucose as a carbon source, *E. coli*-ABC$_{Ah}$ produced less amount of P(3HB) than using glycerol; while, high carbon: nitrogen ratio and the induction at the early exponential growth phase accelerated the ability to synthesize P(3HB) from glycerol by *E. coli*-ABC$_{Ah}$.

Furthermore, the hybrid pathway for biosynthesis of SCL-MCL-PHA copolymers has been established. Co-expressing PhaAB with three different PhaCs and three different PhaJs led to the production of various types of SCL-MCL-PHA copolymers. The copolymers produced consisted of C4 to C10 monomers with various fractions of MCL-units up to 64 mol%. In this study, *in vivo* substrate specificities of two PhaC enzymes from *A. hydrophila* ATCC 7966 (PhaC$_{Ah}$) and *P. putida* KT2440 (PhaC2$_{Pp}$) were identified, i.e. PhaC$_{Ah}$ is specified to C4 and C6 monomers, while PhaC2$_{Pp}$ had broader substrate specificity toward C4 to C10 monomers. Moreover, the results demonstrated that PhaJ from *A. hydrophila* (PhaJ$_{Ah}$) could produce various

types of MCL-monomer, up to C10. Also, the correlation between the molar fraction of MCL-unit and the amount of dodecanoate was demonstrated which was increasing amount of dodecanoate increased molar fraction of MCL-unit.

This work also showed that crude glycerol can be used as a sole carbon source for biosynthesis of P(3HB). *E. coli*-ABC$_{Ah}$ produced P(3HB) at 14 wt% of CDW from 1% (v/v) crude glycerol. *E. coli*-ABC$_{Ah}$J$_{Ah}$ produced P(3HB-*co*-3HHx) copolymer by using crude glycerol supplemented with dodecanoate. Although both recombinant strains (*E. coli*-ABC$_{Ah}$ and *E. coli*-ABC$_{Ah}$J$_{Ah}$) accumulated less % content of PHAs from crude glycerol than pure glycerol, the higher amount of total CDW was obtained from crude glycerol, thus leading to higher PHA concentration (g/L).

Incorporation of 3HHx unit (MCL-unit) in polymer decreased both glass transition temperature (T_g) and melting temperature (T_m) of P(3HB) homopolymer. These properties are superior to P(3HB) homopolymer and are required for ease of melting process.

In my thesis work, I have constructed several recombinant *E. coli* strains for production of PHAs from glycerol and provided information for optimization of higher PHA production yield from glycerol with the designed properties to achieve overall improvement in economic competitiveness in the bio-plastic industry. Moreover, this work will encourage the development of PHA biosynthesis system integrated with biodiesel production to reduce the production cost of PHA and simultaneously reduces the problem of surplus crude glycerol.